PROTEINS: Structure, Function, and Genetics 44:400–417 (2001)

INVITED REVIEW

What Are the Dielectric "Constants" of Proteins and How To Validate Electrostatic Models?

Claudia N. Schutz and Arieh Warshel*
Department of Chemistry, University of Southern California, Los Angeles, California

ABSTRACT **Implicit models for evaluation of electrostatic energies in proteins include dielectric constants that represent effect of the protein environment. Unfortunately, the results obtained by such models are very sensitive to the value used for the dielectric constant. Furthermore, the factors that determine the optimal value of these constants are far from being obvious. This review considers the meaning of the protein dielectric constants and the ways to determine their optimal values. It is pointed out that typical benchmarks for validation of electrostatic models cannot discriminate between consistent and inconsistent models. In particular, the observed pK_a values of surface groups can be reproduced correctly by models with entirely incorrect physical features. Thus, we introduce a discriminative benchmark that only includes residues whose pK_a values are shifted significantly from their values in water. We also use the semimacroscopic version of the protein dipole Langevin dipole (PDLD/S) formulation to generate a series of models that move gradually from microscopic to fully macroscopic models. These include the linear response version of the PDLD/S models, Poisson Boltzmann (PB)-type models, and Tanford Kirkwwod (TK)-type models. Using our different models and the discriminative benchmark, we show that the protein dielectric constant, ε_p, is not a universal constant but simply a parameter that depends on the model used. It is also shown in agreement with our previous works that ε_p represents the factors that are not considered explicitly. The use of a discriminative benchmark appears to help not only in identifying nonphysical models but also in analyzing effects that are not reproduced in an accurate way by consistent models. These include the effect of water penetration and the effect of the protein reorganization. Finally, we show that the optimal dielectric constant for self-energies is not the optimal constant for charge-charge interactions. Proteins 2001; 44:400–417.** © 2001 Wiley-Liss, Inc.

Key words: protein dielectric constants; electrostatic energies; self-energy; ion-pairs in proteins

INTRODUCTION

The importance of electrostatic effects as the primary correlation between structure and function of biological molecules has been pointed out[1–7] and demonstrated[2–7] repeatedly. It is now quite clear that electrostatic effects play a major role in enzyme catalysis,[4,8] electron transfer,[9,10] proton transport,[4,11,12] ion channels,[13,14] ligand binding,[15,16] macromolecular assembly,[1,17] and signal transduction.[18] However, obtaining quantitative correlation requires computational models that capture the microscopic nature of electrostatic effects in the very heterogeneous environment of macromolecules. Here the conceptual problems associated with the proper evaluation of electrostatic energies and the nature of the dielectric constant are far from trivial. Furthermore, the validation of electrostatic models is very problematic. For example, although it has been realized that pK_a values calculations provide an effective way for validating electrostatic models,[3,19,20,21,22,23,24,25] most studies have focused mainly on the pK_a values of surface groups. Unfortunately, these pK_a values can be reproduced by many models, including those that are fundamentally incorrect.[26] Thus, the commonly used benchmarks may lead toward unjustified conclusions about the nature of electrostatic effects in proteins. It has been pointed out[21,26] that ionizable groups in protein interiors should provide a much more discriminating benchmark because these groups reside in very heterogenous environment, where the interplay between polar and nonpolar components is crucial. For example, an ionizable group in a *true* nonpolar environment will have an enormous pK_a shift, and such a shift cannot be reproduced by models that assume high dielectric in the protein interior. Similarly, a model that describes the protein as a uniform low dielectric medium, without permanent dipoles, will not work in cases where the environment around the ionizable group is polar.[3]

Grant sponsor: National Institutes of Health; Grant number: GM-40283.

*Correspondence to: Arieh Warshel, Department of Chemistry, University of Southern California, Los Angeles, CA 90089-1062. E-mail: warshel@invitro.usc.edu

Received 1 February 2001; Accepted 9 April 2001

The meaning of the dielectric constant of proteins has been addressed before[3,26,27] and has become a subject of significant current interest.[6,26,21,27,28,29,30,31] However, important aspects of this issue do not appear to be widely understood, perhaps because of the use of indiscriminating benchmarks and the use of macroscopic concepts for very heterogeneous polar environments. Thus, the use of a proper test case should help in clarifying the nature of the dielectric constants of macromolecules.

This review starts by arranging different electrostatic models in a hierarchical order going from fully microscopic to more and more macroscopic models. As a bridge between these models we will use the semimacroscopic version of the protein dipoles Langevin dipole (the PDLD/S) model. This model provides a unique and direct link between the different models used and thus offers a consistent way of determining the nature of the dielectric constant. After describing the different models, we provide a clear illustration of the difference between discriminative and nondiscriminative benchmarks for validating electrostatic models. Using a proper benchmark allows us to establish the difference between various macroscopic and semimacroscopic models and to illustrate the nature of the protein dielectric constants. In particular, it will be shown that the protein dielectric constants depend on their definition[3] and on which effects are treated explicitly.[32]

METHODS AND CONCEPTS

Using pK_a Values in Studies of Electrostatic Energies in Proteins

To validate electrostatic models in proteins it is useful to consider the energetics of charges in proteins. Relevant test cases include ionization of acidic and basic groups in proteins (or the corresponding pK_a values),[3,19–25] reduction or oxidation processes in redox centers in proteins[10,33,34] and binding of charged ligands.[15,16,35,36] Here we will focus on pK_a values of ionizable groups. Our starting point is the microscopic thermodynamic cycle of Figure 1. This figure considers the free-energy contributions associated with the ionization of an acidic residue in a protein. This cycle, which was first introduced in Ref. 37, gives

$$\Delta G^{p}(AH_p \rightarrow A_p^- + H_w^+) = \Delta G^{w}(AH_w \rightarrow A_w^- + H_w^+) + \Delta G_{sol}^{w\rightarrow p}(A^-) - \Delta G_{sol}^{w\rightarrow p}(AH) \quad (1)$$

where p and w designate protein and water, respectively, and $\Delta G_{sol}^{w\rightarrow p}$ represents the free-energy difference of moving the indicated group from water to its protein site (for more details about the cycle see Ref. 38). This free-energy difference is considered formally as a change in "solvation" free energies. Eq. 1 can be rewritten, for the ith ionizable residue as (see Ref. 37)

$$pK_{a,i}^{p} = pK_{a,i}^{w} - \frac{\bar{q}_i}{2.3\,RT}\,\Delta\Delta G_{sol}^{w\rightarrow p}(AH_i \rightarrow A_i^-) \quad (2)$$

where $\Delta\Delta G$ term consists of the last two terms of Eq. 1. $\bar{q}_i$ is the charge of the ionized form of the given residue, for acids we have $\bar{q}_i = -1$ ($q(AH) = 0$, $q(A^-) = -1$) and for base we have $\bar{q}_i = +1$ ($q(AH) = +1$, $q(A^-) = 0$). To evaluate the free energy of an ionized group in a protein, it is useful and convenient to consider first the self-energy of ionizing this group when all other ionizable groups are uncharged and then to consider the effect of charging the other groups to their given ionization state. Thus, we can express the $\Delta\Delta G_{sol}$ terms of Eq. 2 as

$$\begin{aligned}(\Delta\Delta G_{sol}^{w\rightarrow p})_i &= (\Delta G_{self}^{p} - \Delta G_{self}^{w})_i + \sum_{j\neq i}\Delta G_{ij}^{p} \\ &= (\Delta G_{self}^{p} - \Delta G_{self}^{w})_i + \Delta G_{qq}^{(i)} \\ &= (\Delta G_{q\mu}^{p} + \Delta G_{q\alpha}^{p} + \Delta G_{qw}^{p} - \Delta G_{self}^{w})_i + \Delta G_{qq}^{(i)} \end{aligned} \quad (3)$$

where ΔG_{self} is the self-energy associated with charging the ith group in its specific environment. In the case of a charge in a protein we decompose ΔG_{self} into the free energy of interaction between the charge and its surrounding permanent dipoles ($\Delta G_{q\mu}$) and induced dipoles ($\Delta G_{q\alpha}$) as well with the water molecules in and around the protein (ΔG_{qw}) and $\Delta G_{ij}^{(p)}$ is the free energy of interaction between the ith and jth ionized residues. The actual evaluation of the contributions to ΔG_{sol} is not addressed at this point, but they are clearly free energies rather than energy contributions. Note that the magnitude of the contributions to the total free energy depend on the cycle used and the evaluation of such contributions by free-energy perturbation (FEP) approaches is not additive. Fortunately, however, contributions evaluated by the linear response approximation (LRA) approach are additive.

Eq. 3 can be viewed as the sum of the loss of "solvation" energy associated with removing the charge from water ($-\Delta G_{self}^{w}$) plus the "solvation" of the charge by its surrounding protein environment (the protein dipoles and water molecules) and finally the interaction between the charge and the ionized groups. It is useful to note that the crucial self-energy terms in Eq. 3, which were introduced in ref. 37, were later adopted by other workers[39] and renamed, introducing a cycle that involves a hypothetical nonpolar protein (see Ref. 40 for such a cycle), where the charge is first moved from water to a hypothetical nonpolar environment, without the protein permanent dipoles, followed by activation of the dipoles. In this new notation we have

$$\Delta\Delta G_{self}^{w\rightarrow p} = \Delta G_{self}^{p} - \Delta G_{self}^{w} = \Delta G_{Born} + \Delta G_{back} \quad (4)$$

where the free energy of the first step is denoted by ΔG_{Born}, whereas the interaction between the ionized group and its polar environment has been named "ΔG_{back}". The ΔG_{back} term is given to a reasonable approximation by $\Delta G_{q\mu}/\varepsilon_p$ where ε_p is the assumed dielectric "constant" of the protein (the meaning of this parameter will be discussed in subsequent sections).

In general, we can express the pK_a of each group of the protein by

$$pK_{a,i}^{p} = pK_{app,i}^{p} = pK_{int,i}^{p} + \Delta pK_{a,i}^{charges} \quad (5)$$

where $pK_{int,i}$ is the so-called intrinsic pK_a (this is the pK_a that the ith group in the protein would have when all other

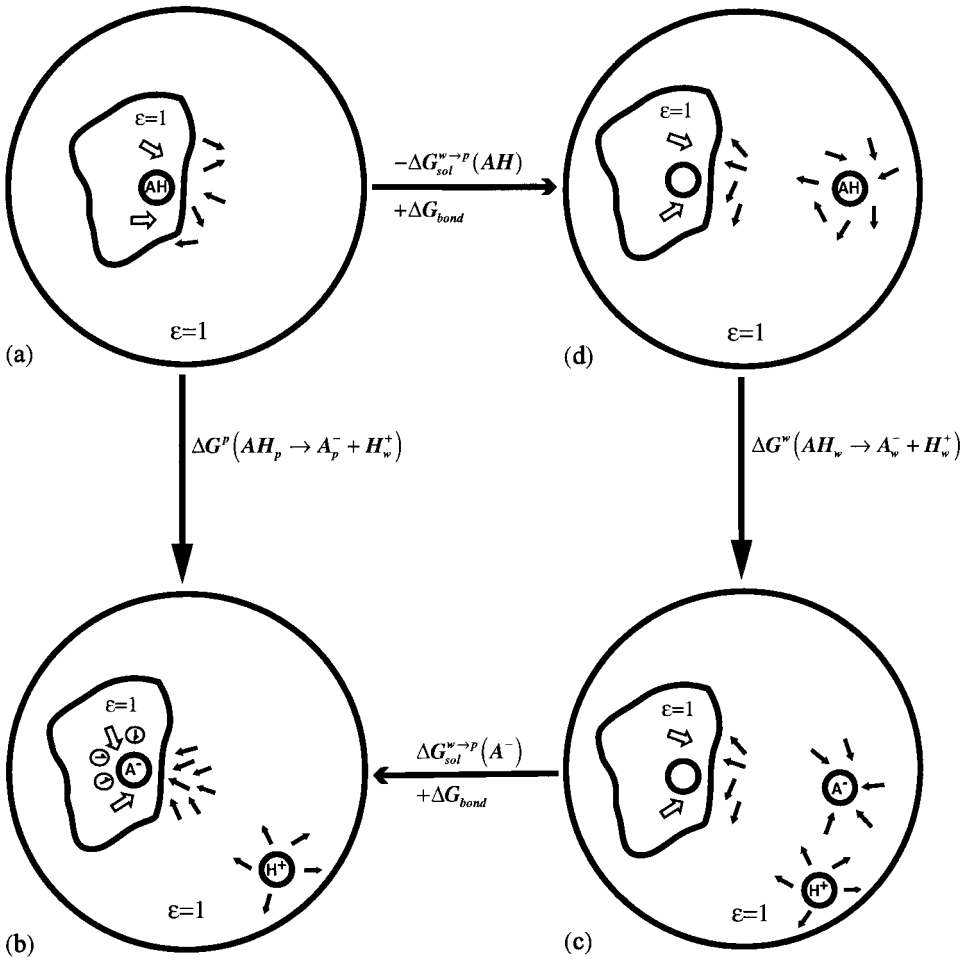

Fig. 1. Thermodynamic cycle for ionization of an acidic group (AH) in a protein active site. The figure describes a fully microscopic cycle and lists the relevant free energy contributions. p and w designate, respectively, protein and water environments. The different solvation free energies are designated by ΔG_{sol}, whereas ΔG_{bond} designates the free energy of breaking the covalent bond between A and the protein. The protein permanent and induced dipoles are designated, respectively, by large open arrows and small arrows inside circles. The polarization of the water molecules is designated schematically by narrow black dipoles. The dipoles drawn are of course schematic and the actual free energy calculation involves the proper LRA averaging on the relevant configurations.

groups are in their neutral states) and $\Delta pK_{a,i}^{charges}$ represents the effects of the other ionized groups ($\Delta pK_{a,i}^{charges} = -(\bar{q}/2.3\,RT)\sum_{j\neq i}\Delta G_{ij}^{p}$). Here we use the notation $pK_{app,i}$ for the actual (apparent) pK_a of the ith group. Using Eqs. 2, 3, and 5 we can write

$$pK_{app,i}^{p} = pK_{a,i}^{w} - \frac{\bar{q}_i}{2.3\,RT}\Delta\Delta G_{self,i}^{w\to p} + \Delta pK_{a,i}^{charges} \qquad (6)$$

where the ΔG_{ij}^{p} represents the interaction with the jth ionized group. Eq. 6 can also be written as

$$\Delta\Delta G_{self,i}^{w\to p} = -\frac{2.3\,RT}{\bar{q}_i}(pK_{app,i}^{p} - \Delta pK_{a,i}^{charges} - pK_{a,i}^{w})$$

$$= -\frac{2.3\,RT}{\bar{q}_i}\Delta pK_{int,i} \qquad (7)$$

The evaluation of $\Delta\Delta G_{self}$ and ΔG_{ij} can be accomplished by microscopic and macroscopic models. The nature of both type of approaches will be considered below.

Microscopic Models

The pK_a values of ionizable groups in proteins can be evaluated by microscopic models that include explicitly all the atoms in the simulation region. The relevant free energies can be evaluated by the simplified solvent model of the protein dipole Langevin dipole (PDLD) method[3,41,38] or by the formally rigorous FEP method.[20,42,43] The FEP results can be estimated conveniently by the LRA,[15,23] which provide a framework for some aspects of our discussion. The LRA method gives ΔG_{self} by[15,44]

$$\Delta G_{self} = \Delta G_{(q=0\to q=q_0)} = \tfrac{1}{2}[\langle\Delta V\rangle_{q=0} + \langle\Delta V\rangle_{q=\bar{q}}] \qquad (8)$$

Here ΔV is the change in potential when q changes from zero to $\bar{q}$. $\langle\ \rangle_q$ designates the average over trajectories with the potential surface of the protein with the designated q. The specific form of the potential surface is irrelevant for the present discussion.

Although the molecular nature of microscopic models is clear, their implementation is far from obvious. In particular, one must face the fact that the simulation involves finite systems and that electrostatic interactions lead to highly correlated long-range effects. Periodic boundary conditions and the Ewald sum approach do not capture the radial symmetry around charges.[45,46] Corrections terms for the Ewald treatment exists in some cases (e.g., Refs. 47 and 48), but it is not clear if such corrections work in proteins (see discussion in Ref. 45). A possible solution is to treat solvation problems by spherical models. Here, however, one must represent correctly the effect of the system that is not treated explicitly. The problem is not in the well-known bulk contributions from the surrounding of the simulation sphere,[3,49] which has been implemented repeatedly in computational studies (e.g., Refs. 44 and 50), but in the requirement of having a proper polarization for the surface molecules of the explicit system.[3] A solution to this problem has been introduced by one of us,[51] who developed for this purpose special polarization constraint. This idea has been refined in subsequent works and led to the surface constraint all-atom solvent (SCAAS) model (e.g. Ref. 52). However, widely used simulation approaches that involved spherical models (e.g. Ref 53) focus on the less-relevant issue of keeping the proper temperature at the boundaries (which is accomplished by many thermalization methods) and overlooked the need to have proper electrostatic boundaries. Some advances in realizing this problem have been made in a recent study,[54] which adapted the crucial SCAAS idea of the angular constraint. Unfortunately, the angular constraint was presented as a trivial well-known idea and the rather obvious treatment of the bulk effect was featured as a significant advance. In fact, the response of the bulk to an explicit spherical system is well known and have been used repeatedly before (e.g. Refs. 3, 44, 45, 50). What is much less appreciated and not recognized in text books is the problems with the boundaries between the explicit and bulk regions.[51] At any rate, most simulation studies do not yet use proper surface polarization.

Another problem is the treatment of long-range effects. Here again an effective treatment was introduced with the local reaction field (LRF) model.[42] However, most spherical models still involve cutoff treatments that tends to lead to overpolarization of the solvent (see discussion in Refs. 45, 51, and 55). In addition to the above problems, one faces the fact that microscopic calculation of electrostatic free energies involve major convergence problems. Because of these reasons there are only limited microscopic evaluations of pK_a values in proteins (e.g. Refs. 3, 20, 23, 38, 44). At present, the results of such microscopic calculations are not completely satisfactory and they also require major simulation time. Furthermore, the use of macroscopic models with nondiscriminative benchmark (see Establishing a Meaningful Benchmark) probably gave the impression that such models are more reliable than microscopic models and that this reliability reflects some fundamental physics. Thus, most practical studies involve implicit models whose nature is the subject of the present work. It should be recognized, however, that the clear physical insight of the microscopic models has been very useful in providing understanding of the nature of electrostatic energies in proteins[3,41] (much before the emergence of such understanding from macroscopic studies). Furthermore, the microscopic studies were crucial in pointing out the problems with the early macroscopic models and in clarifying the nature of the dielectric constant of proteins.[3,26] In fact, the connection between the microscopic and macroscopic pictures will be our guide in this review.

Bridging Microscopic and Macroscopic Models

Macroscopic and semimacroscopic models represent the protein by assumed dielectric constants. To determine the nature of this constants, it is essential to use a formulation that transforms the microscopic picture to the corresponding macroscopic picture. Because we deal with very heterogenous environment, we cannot use the standard relationship between the dipole fluctuations and the dielectric constant to determine the protein dielectric constant (see The Nature of ε_p). A proper formulation must lead to the actual expression used in the analyzed macroscopic treatment. A formulation that satisfies this requirement is the PDLD/S model.[38,40,44] This model allows one to map a fully microscopic model into different semimicroscopic model and to have a well-defined relationship between these models. As will be shown below, the PDLD/S provide a continuous transformation from the fully microscopic PDLD-LRA treatment to more and more macroscopic models. Thus, we start the subsequent discussion by introducing the PDLD/S formulation as a basis and guide for the subsequent analysis.

The PDLD/S model is based in the thermodynamic cycle of Figure 2. This cycle considers, as an example, the change in solvation of A^- on transfer from water to the protein site ($\Delta G^{w\rightarrow p}_{sol}(A^-)$). The protein is described as a medium with a dielectric constant ε_p, but with an explicit description of the protein permanent dipoles. The cycle of Figure 2 involves the change of the solvent dielectric from the dielectric constant of water ($\varepsilon = \varepsilon_w = 80$) to $\varepsilon = \varepsilon_p$, transferring the charges to the protein and finally changing back the dielectric of the solvent to ε_w. These processes give the total free energy, $\Delta G_{a\rightarrow b}$, by

$$\Delta G_{a\rightarrow b} = \Delta G_{a\rightarrow d} + \Delta G_{d\rightarrow c} + \Delta G_{a\rightarrow b} \tag{9}$$

As explained in Appendix A the sum of these three terms is given by

$$\Delta V^{w\rightarrow p}_{pdld/s,i} = \Delta G_{a\rightarrow b} \simeq [\Delta\Delta G^w_p(q_i = 0 \rightarrow q_i = \bar{q}_i) - \Delta G^w_{q,i}]\left(\frac{1}{\varepsilon_p} - \frac{1}{\varepsilon_w}\right) + \frac{\Delta V^p_{q\mu}(q_i = \bar{q}_i)}{\varepsilon_p} \tag{10}$$

where ΔG^w_q is the self-energy of the given charge in water (our ΔG^w_{self}), the $\Delta\Delta G^w_p$ term represents the change in the microscopic solvation energy of the entire protein (plus its bound ionizable group) upon changing the charge of this group from zero to $\bar{q}$. $\Delta V_{q\mu}$ is the potential energy term that would become $\Delta G_{q\mu}$ upon averaging. Note that we consider the charge–charge interaction (the ΔG_{ij} term)

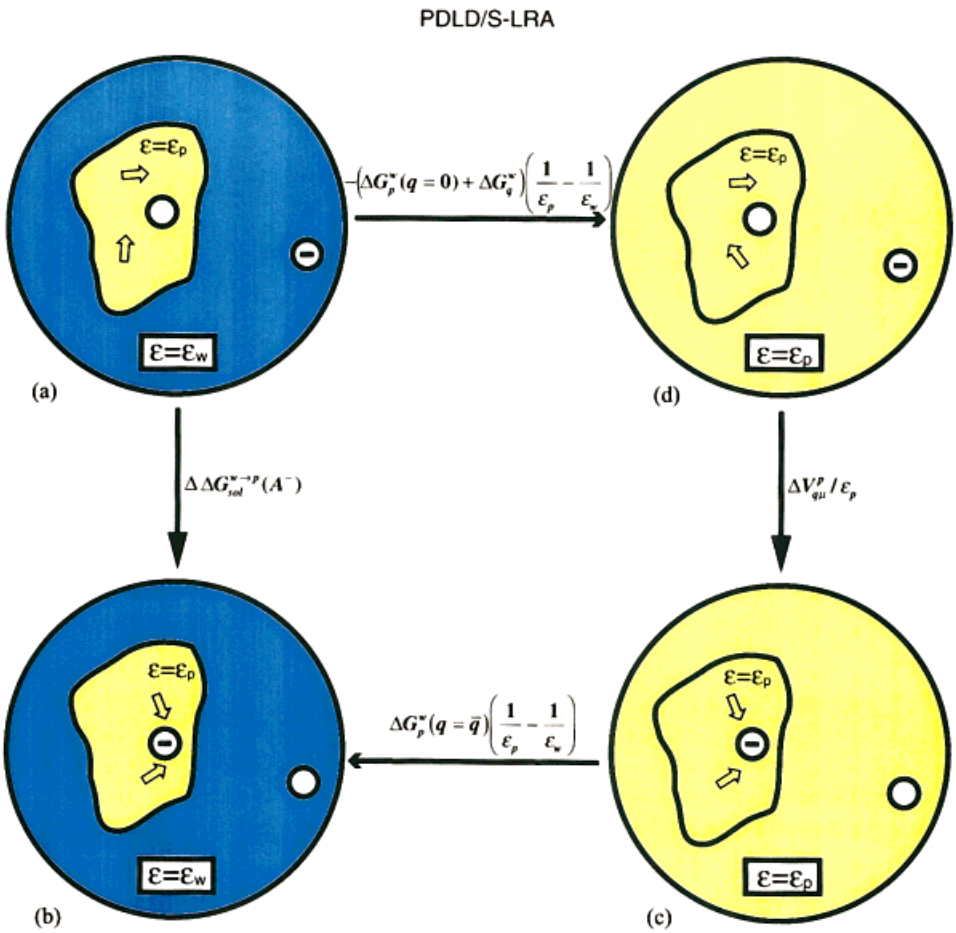

Fig. 2. The PDLD/S-LRA thermodynamic cycle for the evaluation of $\Delta\Delta G_{sol}^{w\rightarrow p}(A^-)$. The cycle involves the change of the dielectric constant of the solvent around the protein from ε_w to ε_p, moving the charge from the solvent to the protein, changing back to the solvent dielectric and uncharging the ionized group inside the protein. The energy contribution of each step is indicated in the figure (see text). The LRA process is designated by the reorientation of the protein permanent dipoles.

separately. The origin of the $\left(\frac{1}{\varepsilon_p} - \frac{1}{\varepsilon_w}\right)$ scaling is explained in Appendix A.

In the case of the PDLD/S model, the solvent is represented by a grid of Langevin Dipoles (LD) which follow the Langevin polarization law (see Refs. 38 and 44). The PDLD/S-LRA method obtains the relevant free energy by using Eq. 8 with the ΔV of Eq. 10. That is, in this model we use

$$\Delta G_{pdld/s} = \tfrac{1}{2}\left[\langle \Delta V_{pdld/s}\rangle_{q=0} + \langle \Delta V_{pdld/s}\rangle_{q=\bar{q}}\right] \qquad (11)$$

where $\langle\ \rangle_q$ designates an average over protein configurations generated with the protein force field and the indicated charge state (q). Here $\Delta V_{pdld/s}$ is the ΔV of Eq. 10. In other words, to obtain the relevant free energy, we evaluate the PDLD/S energy of an ionized group by averaging it over configurations generated with the charge of this group set to its full final value ($q = \bar{q}$) and to its initial neutral value ($q = 0$).

The remarkable property of the combination of Eqs. 9 and 10 is that all the quantities that are scaled by $(1/\varepsilon_p - 1/\varepsilon_w)$ are microscopic quantities with a clear molecular meaning. Moreover, once ε_p becomes unity, we obtain the fully microscopic free energy for a model without induced dipoles (no $\Delta G_{q\alpha}$). With the induced dipoles effect we can reproduce the microscopic picture by using $\varepsilon_p = 2$ (see Ref. 3). What we have now is a development of a basic equation for converting microscopic treatments to semimacroscopic treatments. Obviously, there is no way of going in the opposite direction and converting macroscopic or semimicroscopic treatments to microscopic treatments.

Semimacroscopic Models

With the PDLD/S-LRA model we can start to formulate less and less microscopic approaches. First, ignoring the LRA treatment of Eq. 11, we obtain the PDLD/S expression (Eq. 10). This model reproduces the main ingredients of the descritized continuum (DC) or Poisson Boltzmann (PB) approaches,[5] but with a much clearer physical origin. That is, modern PB treatments represent the solvent and the protein by continuum models while considering the effect of the protein dipoles (the $V_{q\mu}$ term) explicitly.

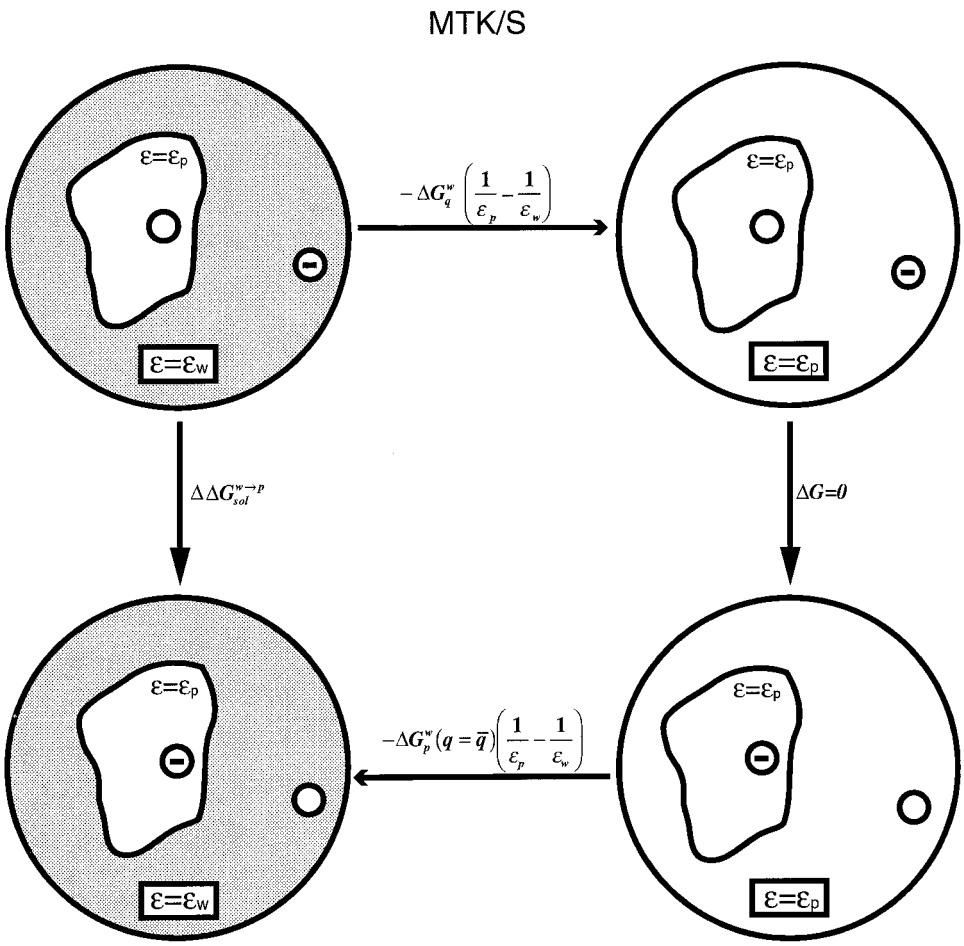

Fig. 3. The MTK(S) thermodynamic cycle. This cycle is identical to the PDLD/S cycle except that the crucial effect of the protein permanent dipoles is ignored.

Replacing the solvent contribution (the ΔG_p^w values term) by the corresponding continuum results gives basically the same results as that of current PB methods. Note in this respect, that the averaging of the PB results over protein configurations generated with $\bar{q}$, does not yet correspond to the proper LRA treatment (which requires also an average over configurations generated with $q = 0$).

Macroscopic Models

After clarifying the basis of the semimacroscopic model, we can move to fully macroscopic models. Here the crucial step is the removal of the "back field" term. This important $V_{q\mu}$ term has been missing in all early continuum treatments but is now implemented in most PB treatments. The omission of the protein permanent dipoles has been frequently presented as a minor technical issue, implying[56] that these dipoles are simply missing protein charges, which are not different from the protein ionized groups (which have been considered in all early models). This implication involves, however, a fundamental inconsistency where the permanent dipoles of the system, whose relaxation is a major part of the dielectric effect of the system, are considered on the same level as the charges in this system. This philosophy is akin to representing water as a collection of charges immersed in a low dielectric. At any rate, models that neglect $V_{q\mu}$ give

$$\Delta\Delta G_{self,i}^{w\to p} \Rightarrow \Delta\Delta G_{MTK(S),i}^{w\to p}$$

$$\Delta\Delta G_{MTK(S),i}^{w\to p} = [\Delta\Delta G_p^w(q_i = 0 \to q_i = \bar{q}_i) - \Delta G_{q,i}^w]\left(\frac{1}{\varepsilon_p}-\frac{1}{\varepsilon_w}\right) \quad (12)$$

Here we used the notation MTK(S) to designate that the expression used corresponds to the modified Tanford Kirkwood (MTK) model,[57] but the protein is treated with its actual structures (shape) rather then as a sphere (see Fig. 3). In this model we are not using the LRA so that our results represent free energy rather than an effective potential. The actual MTK model with a spherical protein (Fig. 4) gives

$$\Delta\Delta G_{self,i}^{w\to p} \Rightarrow \Delta\Delta G_{MTK,i}^{w\to p}$$

$$\Delta\Delta G_{MTK,i}^{w\to p} \cong -166\left(\frac{1}{b}+\frac{r_i^2}{b^3}\right)\left(\frac{1}{\varepsilon_p}-\frac{1}{\varepsilon_w}\right)+\left(\frac{166}{\bar{a}_i}\right)\left(\frac{1}{\varepsilon_p}-\frac{1}{\varepsilon_w}\right) \quad (13)$$

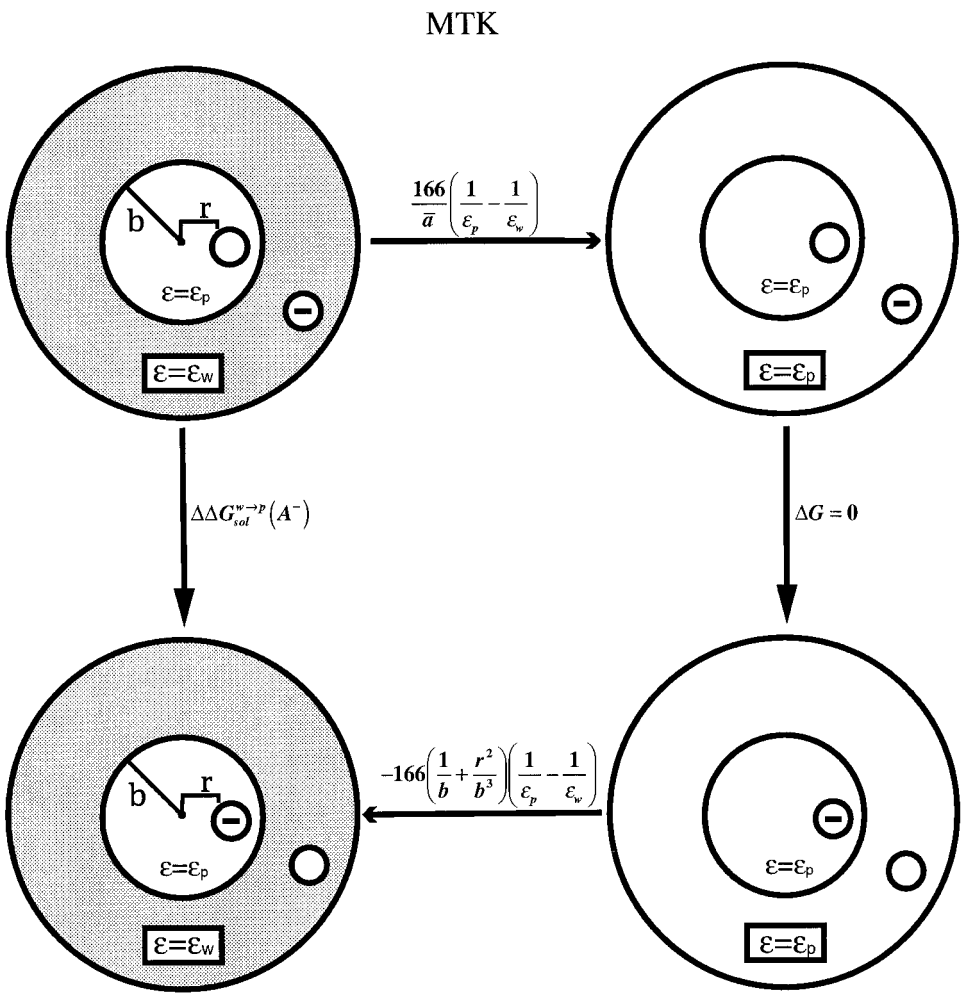

Fig. 4. The MTK thermodynamic cycle. Here the protein is represented by a sphere of a radius b.

where the ΔG is given in kcal/mol and the different radii in Å. Here $\bar{a}_i$ is the Born's radius of the ith charged group, b is the effective protein radius, and r_i is the shift of the position of the charged group from the center of the protein (see Fig. 4). Also note that the $(1/\varepsilon_p - 1/\varepsilon_w)$ is an approximation for the correct scaling of the dipole term (see Appendix A).

The next approximation is the original Tanford Kirkwood (TK) approximation, which gives[57,58]

$$\Delta\Delta G_{self,i} \Rightarrow \Delta\Delta G_{TK,i}$$

$$\Delta\Delta G_{TK,i} \cong -166\left(\frac{1}{b}+\frac{r_i^2}{b^3}\right)\left(\frac{1}{\varepsilon_p}-\frac{1}{\varepsilon_w}\right) \tag{14}$$

Here, in contrast to common belief, we do not have the Born's term, which was evidently neglected (see discussion in Ref. 57) because it was thought at that time that all ionized groups must reside on the surface of the protein. In this case, we cannot use the notation $w \to p$ because we are not dealing with the energy of transferring the given residue from water to protein but the free energy of changing the dielectric of the solvent from ε_p to ε_w.

Finally, some workers,[59] have considered the approximation

$$\Delta\Delta G^{w\to p}_{self,i} \Rightarrow \Delta\Delta G^{w\to p}_{Born(\infty),i}$$

$$\Delta\Delta G^{w\to p}_{Born(\infty),i} = \left(\frac{166}{\bar{a}_i}\right)\left(\frac{1}{\varepsilon_p}-\frac{1}{\varepsilon_w}\right) \tag{15}$$

This model neglects the effect of the water around the protein, so that we basically have an infinitely large protein.

At this point, we may consider the evaluation of the charge–charge interaction terms (the $\Delta G^{(i)}_{qq}$ of Eq. 3). Formally, the simplest way is to evaluate the interaction with other ionized groups by adding explicitly the corresponding V^p_{qq} term to the $V^p_{q\mu}$ term of Eq. 10. The actual ionization state of each residue at the given pH can then be evaluated self-consistently by a Monte Carlo or related approaches (see, e.g., Refs. 38, 39, and 60). However, using a Monte Carlo treatment with repeated PDLD/S-LRA calculations or with PB calculations is very expensive. Thus, it is more reasonable to have a general estimate of

the interaction between each pair of residues. This can be done by using

$$\Delta G^{p}_{ij} = \Delta G(q_i = 0 \rightarrow q_i = \bar{q}_i)_{q_i = \bar{q}_j} - \Delta G(q_i = 0 \rightarrow q_i = \bar{q}_i)_{q_j = 0} = \bar{q}_i \bar{q}_j W_{ij} \quad (16)$$

and then expressing W_{ij} by

$$W_{ij} = \frac{332}{r_{ij}\varepsilon_{ij}} \quad (17)$$

In this direct treatment ε_{ij} is a function of ε_p, but it is unlikely that the ε_p for charge-dipole and charge–charge interactions are identical (see below). Therefore, it might be preferable to consider ε_{ij} as an independent dielectric for charge–charge interaction (now ε_{ij} represents the effect of ε_p, the effect of the protein reorganization and the effect of the solvent). In general, it is found that ε_{ij} can be approximated by a large number between 20 and 80 or by a distance-dependent function of the form[57]

$$\varepsilon_{ij} = \varepsilon_{eff} = 1 + \varepsilon'(1 - \exp\{-\mu r_{ij}\}) \quad (18)$$

as well as by related functions.[61]

Finally, we should also mention the so-called "Generalized Born" (GB) model. Although this model is sometimes presented as a fundamental model for interacting charges[62] it is basically the result of assuming a medium with a uniform dielectric.[3,63] That is, in a medium of a uniform dielectric, ε_{GB}, we may write the free energy of two interacting charges as the sum of the gas-phase energy plus the solvation energy. We can also write this free energy as the sum of the solvation energy at infinity and the energy of bringing the charges together from infinity to R_{ij} in solution.[3] These two alternative formulations give

$$\Delta G^{GB}_{ij}(R_{ij}) = 332\,\frac{\bar{q}_i\bar{q}_j}{R_{ij}} + \Delta G^{GB}_{sol}(R_{ij}) = \Delta G^{\infty}_{sol} + 332\,\frac{\bar{q}_i\bar{q}_j}{R_{ij}\varepsilon_{GB}} \quad (19)$$

This equation gives

$$\Delta G^{GB}_{sol}(R_{ij}) = -332\,\frac{\bar{q}_i\bar{q}_j}{R_{ij}}\left(1 - \frac{1}{\varepsilon_{GB}}\right) + \Delta G^{\infty}_{sol} = -332\,\frac{\bar{q}_i\bar{q}_j}{R_{ij}}\left(1 - \frac{1}{\varepsilon_{GB}}\right) - 166\left(\frac{\bar{q}_i^2}{\bar{a}_i} + \frac{\bar{q}_j^2}{\bar{a}_j}\right)\left(1 - \frac{1}{\varepsilon_{GB}}\right) \quad (20)$$

where we replaced ΔG^{∞}_{sol} by the corresponding Born's terms. Modern GB treatments (e.g., Ref. 64) modify Eq. 20 by introducing the assumption that ε_{GB} decreases at short distances, which is represented by using

$$\Delta G^{GB}_{sol} = \left[-332\,\frac{\bar{q}_i\bar{q}_j}{(R^2_{ij} + \bar{a}^2_{ij}e^{-D_{ij}})^{1/2}} - 166\left(\frac{\bar{q}_i^2}{\bar{a}_i} + \frac{\bar{q}_j^2}{\bar{a}_j}\right)\right]\left(1 - \frac{1}{\varepsilon_{GB}}\right) \quad (21)$$

where $\bar{a}_{ij} = (\bar{a}_i\bar{a}_j)^{1/2}$ and $D_{ij} = R^2_{ij}/(2\bar{a}_{ij})^2$. It is important to keep in mind, however, that the GB is basically a "glorified" Coulomb's law, which uses as a reference the solvation energies at infinite separation in a medium with $\varepsilon = \varepsilon_{GB}$. Furthermore, a serious problem of the GB model in proteins is the fact that we are dealing with two environments (water and protein). This problem has been overlooked by many workers who perhaps assumed that the GB represents a fundamental insight or that the e^{-D} scaling can properly account for the transition between different environments.

Now after defining all the above models, we are ready to examine their performance in well-defined test cases.

ESTABLISHING A MEANINGFUL BENCHMARK

Although pK_a calculations provide a powerful way for validating electrostatic models, most of the benchmarks used for this purpose have been somewhat misleading. That is, as pointed out long ago,[57] almost any model will give reasonable results for surface groups because the pK_a values of such groups is close to the corresponding values in water. Even a model that assumes zero pK_a shifts (i.e., the null model) will look as an excellent model. In fact, Warshel and coworkers[57] have shown that any model with a large dielectric constant for charge–charge interactions will usually look like an excellent model in cases of surface groups. This observation was also made subsequently by Antosiewicz et al.,[24] who overlooked, however, the point of Ref. 57 that the success of oversimplified models is an illustration of the use of inappropriate benchmark. To illustrate our point it is important to examine the inherent problem of using a nondiscriminative benchmark (NBM), which gives equal weight to all observed pK_a values. As is shown in Figure 5, taking an NBM for acidic and basic surface groups gives the impression of an excellent results for any model that uses a large ε but we also include a few points with smaller ΔpK_a values. Here all the Asp and Glu residues have $pK_a \approx 4$ and all the Lys have $pK_a \approx 10$. Obviously, with these two points we obtain an impressive straight line. However, when we convert the pK_a values to ΔpK_a values, it becomes clear that we are dealing with very little relevant information, because all the ΔpK_a are close to zero and the trivial null model will reproduce this observation. Now, once we consider only groups with large pK_a shifts, we obtain a fundamentally different picture, where the inherent problems of improper models can be detected and analyzed.

Here we define as a discriminative benchmark (DBM) the data set obtained mainly from groups with $|\Delta pK_a| > 2$, but we also include a few special cases with smaller ΔpK_a. Our current set is compiled in Table I. Although this is a limited set, and adding more reliable data points would be very useful, we will be able to make our main points by using the current set.

EXAMINING MACROSCOPIC AND SEMIMACROSCOPIC MODELS

The Self-Energy Term

With our DBM we can now examine the performance of different models. A very instructive analysis should be obtained by removing the effect of the interaction between ionized residues (the $\Delta G^{(i)}_{qq}$ term) and focusing on the self-energy term. To do so, we define a benchmark that

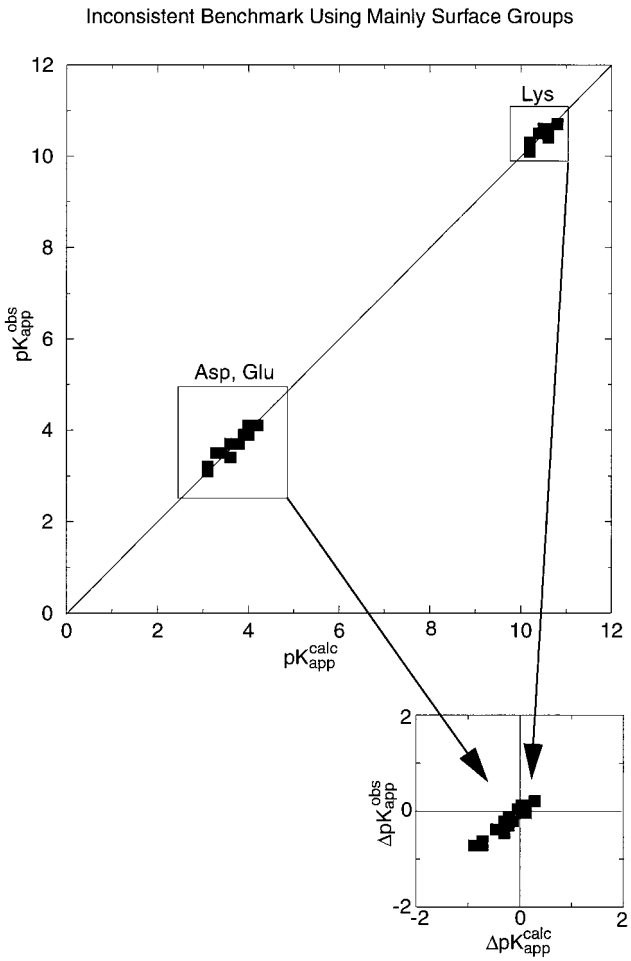

Fig. 5. The correlation between the calculated and observed pK_a values a nondiscriminative benchmark that only involves surface groups. The figure considers Asp, Glu, and Lys residues on the surfaces of Lysozyme and Ribonuclease but includes only those residues with $pK_{app}^{obs} < 1$. The calculated pK_a values are evaluated by the MTK(S) model with $\varepsilon_p = 40$ and $\varepsilon_{eff} = 80$. As seen from the figure, we obtain seemingly impressive results for this benchmark, but when the results are displayed as ΔpK_a, it becomes clear that we have simply a poor benchmark where $\Delta pK_a \simeq 0$ and any model that produces small pK_a shift looks as an excellent model.

contains the best estimate of the "observed" intrinsic pK_a values. This is done by using Eq. 5 and writing

$$\Delta pK_{int,i}^{obs} = (pK_{app,i}^{obs} - \Delta pK_{a,i}^{charges}) - pK_{a,i}^{w}$$
$$= \left(pK_{app,i}^{obs} + \frac{\bar{q}_i \Delta G_{qq}^{(i)}}{2.3\,RT}\right) - pK_{a,i}^{w} \qquad (22)$$

where $\Delta G_{qq}^{(i)}$ is the best calculated estimate of $\Delta G_{qq}^{(i)}$. Here we define $\Delta pK_{int,i}^{obs}$ as an "observed" quantity because the estimate of ΔG_{qq} can be quite reliable. Nevertheless, we also report the results for different estimates of ΔG_{qq}, where the ΔpK_{app} is compared to the corresponding ΔpK_{app}^{obs}.

In our comparative study we try first to look for the ε_p that reproduces the given ΔpK_{int}^{obs} and examine the trend in the resulting ε_p. In a later stage we will take the most common ε_p for each model and examine the predicted ΔpK_{int}. When we search for the optimal ε_p of each model, we will not look for an exact value that satisfies the given equation but consider the best result for discrete values of ε_p (i.e., 2, 4, 6, 8, 20, 40, and 80). In cases of tight ion pairs, it is obviously not justified to consider ΔpK_{int} in simplified models that do not include the counter ion. Thus, in cases where the contribution to $\Delta G_{qq}^{(i)}$ from a given residue (the jth residue) is larger than 2 kcal/mol for the optimal ε_{eff}, we treat this residue explicitly in the PDLD/S calculations and consider the system as an ion-pair system (see Tight Ion Pairs). All the studies reported in this work were performed by using the program POLARIS module[44] of the general simulation package MOLARIS.[65]

Our study starts with one of the simplest and least physical models, where the protein is represented by a uniform dielectric ε_p and an infinite radius. Using this model (Eq. 15) we obtain the results summarized in Table II under *Born*(∞). As seen from the table we need to assume that ε_p is very large (a value between 10 and 20) to reproduce the observed results when the protein destabilizes the ionized residue. Furthermore, we have to use a negative ε_p when the protein stabilizes an ionized group more than water does (e.g., Asp 76 in ribonuclease T1). Obviously, this model misses both the stabilizing effect of the solvent around the protein and the stabilizing effect of the protein permanent dipoles. Of course, as we argued repeatedly (e.g. Refs. 3, 57) neglecting the $V_{q\mu}$ effect prevents one from correctly modeling cases where the protein stabilizes isolated charges.

Next we examine the TK model (Eq. 14). Here the effective protein radii, b, is taken as the distance from the given residue to the surface, although other approximations are possible. Now the results are quite problematic, where in most cases we have to use a negative dielectric constant in order to reproduce the observed ΔpK_a. The reason for this is quite obvious. That is, the TK model does not have a self-energy term, and it only represents the stabilizing effect of changing the dielectric of the solvent from ε_p to ε_w. Thus, whenever the given group is destabilize by the protein we have to use a negative ε_p. Because the TK model does not have any term that reflects the actual radii of the given residue, it would predict the same ΔpK_a for any residue at the same site (e.g., the same $|\Delta pK_a|$ for tyrosine with a large $\bar{a}$ and aspartic acid with small $\bar{a}$). In fact, omitting the self-energy term would have led to enormous errors, if we could really place an ionized residue with a small radius (e.g., aspartate) in the interior of a truly nonpolar protein (see footnote 86 in Ref. 38). However, the interior of a real protein cannot generate a true nonpolar environment around an ionized group, because the protein will either reorient its own polar groups or allow water molecules to penetrate and to stabilize the charges.[3] It is important to realize that the TK model gives reasonable results for the interactions between ionized groups on the surfaces of proteins.[57] Thus, the deficiencies of this model cannot be deduced without considering cases with significant shifts in the intrinsic pK_a values.

Next, we consider the MTK and MTK(S) models that correspond to Eqs. 13 and 12, respectively. These models

TABLE I. Groups Included in Our Benchmark and the Corresponding Observed ΔpK_a Values

Case	Protein	Residue	Notation	ΔpK_a^{obs}	Source	PDB
1	Thioredoxin	Asp 26	thrxD26(o)	3.50	[85]	[86]
2	Thioredoxin	Asp 26	thrxD26(r)	5.30	[85]	[86]
3	cytochrome c	His 26	cytcH26	−3.40	[87]	[88]
4	Staph. Nuclease	Lys 66	SNaseK66	−4.90	[21]	[89]
5	Staph. Nuclease	Glu 66	SNaseE66	4.30	[29]	[29]
6	lysozyme	Glu 35	lysE35	1.80	[90]	[91]
7	T4-lysozyme	Glu 105	T4lysE105	1.50	[92]	[92]
8	T4-lysozyme	Lys 102	T4lysK102	−3.90	[93]	[93]
9	T4-lysozyme	His 31	T4lysH31	2.60	[94]	[93]
10	T4-lysozyme	Asp 70	T4lysD70	−3.40	[94]	[93]
11	erabutoxin	His 6	eraH6	−3.75	[95]	[96]
12	subtilisin inhibitor	His 43	subInH43	−3.35	[97]	[98]
13	Ribonuclease T1	Asp 76	RiboD76	−3.40	[99]	[100]
14	Ribonuclease T1	His 40	RiboH40	1.40	[101]	[100]

TABLE II. Calculated ΔpK_{int} for Different Models[†]

System	Born (∞)	TK	MTK	MTK/S	PDLD/S-A	PDLD/S-B	PDLD/S-LRA	ΔpK_{int}^{obs}	ΔpK_{app}^{obs}
thrxD26(o)	2.2 (20)	3.2 (−4)	2.9 (20)	3.3 (6)	3.1 (4)	3.3 (4)	3.2 (4)	3.2	3.5
thrxD26(r)	5.1 (10)	3.2 (−4)	4.1 (10)	4.0 (6)	3.4 (4)	3.9 (6)	4.6 (4)	4.2	5.3
lysE35	2.2 (20)	2.6 (−10)	3.1 (10)	1.9 (8)	1.9 (4)	2.6 (4)	2.3 (4)	2.3	1.8
T4lysE105	2.1 (20)	2.1 (−40)	0.6 (4)	1.1 (20)	0.7 (2)	1.3 (8)	2.1 (4)	2.0	1.5
T4lysK102	−2.1 (20)	−4.4 (−4)	−3.5 (10)	−4.2 (8)	−3.1 (4)	−3.7 (6)	−3.3 (4)	−2.9	−3.9
eraH6	−1.9 (20)	−2.1 (−10)	−1.2 (20)	−1.9 (8)	−1.6 (4)	−1.0 (20)	−2.1 (4)	−2.1	−3.8
subInH43	−1.9 (20)	−2.5 (−8)	−3.0 (10)	−3.4 (8)	−2.7 (4)	−2.6 (8)	−3.3 (4)	−2.8	−3.4
cytcH26	−1.7 (20)	−1.5 (−30)	−1.8 (6)	−1.5 (8)	−1.4 (4)	−1.9 (8)	−1.4 (6)	−1.6	−3.4
SNaseK66	−5.1 (10)	−3.1 (−4)	−4.1 (10)	−4.4 (8)	−3.3 (4)	−5.0 (8)	−4.4 (6)	−4.8	−4.9
SNaseE66	5.0 (10)	3.3 (−6)	4.4 (8)	4.4 (6)	3.0 (4)	4.6 (6)	3.6 (6)	4.1	4.3
RiboD76	−1.7 (−60)	−1.7 (10)	−2.1 (−25)	−1.5 (−15)	−1.3 (20)	0.2 (80)	−1.3 (4)	−1.8	−3.4

[†]The different models are defined in the text. The optimal ε_p for each model are given in brackets. The reference pK_a^w used are 3.9, 4.3, 6.5, and 10.4 for Asp, Glu, His and Lys, respectively.

have the same problems as the Born's model, because both neglect of the crucial effect of the protein dipoles. When the protein destabilizes charges we need to use a large ε_p, and when the protein stabilizes isolated charges we need a negative ε_p.

Now we move to the PDLD/S model of Eq. 10. Here the results are more uniform. However, the use of the PDLD/S without the LRA treatment is still problematic, because it is not clear what protein structure should be used. If we use the X-ray structure or structures generated by MD simulations with the uncharged forms of the ionizable residues (PDLD/S-B), we will not get the correct stabilization by the protein dipoles and we will have to use a relatively large ε_p. On the other hand, if one uses structures evaluated by MD simulations with the charged form of the ionizable residues (PDLD/S-A), we get overstabilization and sometimes even obtain $\varepsilon_p = 2$. The problems of the PDLD/S model occur, of course, in current PB treatments, because these models do not use the LRA formulation and do not take the protein reorganization into account. The PDLD/S-LRA results of Eq. 11 reflect the use of the most consistent semimacroscopic model. Here we can use $\varepsilon_p = 4$ in most cases and $\varepsilon_p = 6$ in a few cases that are discussed in The Nature of ε_p.

Including Charge–Charge Interactions

Until now we focused on the intrinsic pK_a values of our benchmark set. This was done by using Eq. 22, where we subtract from the apparent pK_a values our best estimates of the corresponding charge–charge interaction term. Now we are ready to discuss the actual apparent pK_a values and the corresponding ΔpK_{app}. In this work we evaluate the apparent pK_a using Eq. 5 and 17, plus a self-consistent evaluation of the ionization states of all the residues. This is done for all cases except in cases where we have tight ion pairs (which will be considered in Tight Ion Pairs).

Before we consider the actual calculations, it might be useful to explain why we use in most cases the ε_{eff} of Eq. 18 (rather than explicit PDLD/S calculations of the second term of Eq. 16) in evaluating the ΔG_{ij} terms. Our approach is based on the following points. First, mutation of charged residues indicated repeatedly that the use of a large ε_{eff} or Eq. 18 is an excellent approximation. Second, a systematic PDLD/S-LRA study of the ΔG_{ij} values in a bacterial reaction center,[28] obtained basically the same results while using Eq. 16 with $\varepsilon_p = 4$ and while using Eq. 17 with a large ε_{eff}. Of course, we could have used here the same approach as in Ref. 28, but this extra effort is not justified. Finally, our systematic study[28] has shown that

TABLE III. The Dependence of the Calculated ΔpK_{app} on ε_p (Rows) and ε_{eff} (Columns)[†]

		4	6	8	20			4	6	8	20
thrxD26(r)	20	7.7	4.4	3.7	2.2	T4lysK102	20	−7.2	−5.2	−4.7	−3.2
5.3	40	6.7	3.9	3.0	1.5	−3.9	40	−5.3	−4.2	−3.5	−1.7
	80	**5.7**	3.4	2.7	1.2		80	**−4.3**	−3.2	−2.5	−1.5
		4	6	8	20			4	6	8	20
thrxD26(o)	20	4.5	3.4	2.5	1.8	cytcH26	20	−9.4	−8.4	−7.9	−7.6
3.5	40	3.7	2.9	2.2	1.4	−3.4	40	−6.9	−4.8	−4.4	−3.9
	80	**3.5**	2.4	1.7	0.9		80	−4.1	**−3.2**	−2.9	−2.2
		4	6	8	20			4	6	8	20
subInH43	20	−2.1	−0.3	0.9	1.9	eraH6	20	−6.3	−6.3	−6.3	−5.8
−3.4	40	−2.9	−1.3	−0.6	0.6	−3.8	40	−5.3	−4.3	−3.8	−3.3
	80	**−3.9**	−1.8	−1.1	−0.1		80	**−3.8**	−2.8	−2.3	−1.8
		4	6	8	20			4	6	8	20
SNaseE66	20	5.9	3.3	2.1	0.1	SNaseK66	20	−7.5	−5.6	−3.5	1.9
4.3	40	5.8	3.6	2.6	0.6	−4.9	40	−7.7	−4.5	−3.0	−0.3
	80	5.6	**3.8**	2.8	1.1		80	−7.0	**−4.5**	−3.0	−0.8
		4	6	8	20			4	6	8	20
T4lysE105	20	0.1	−1.1	−1.4	−4.6	lysE35	20	2.0	−0.5	−1.1	−4.1
1.5	40	1.1	0.4	0.1	−2.6	1.8	40	1.1	0.5	0.1	−1.7
	80	**1.6**	1.0	0.6	−1.6		80	**1.8**	1.0	0.6	−0.2

[†]The observed values are given below the entry of the corresponding results. The best calculated values are given in bold numbers.

the PDLD/S approach without the LRA treatment (which is equivalent to the corresponding PB treatments) requires one to use quite frequently a relatively large ε_p ($\varepsilon_p \rightarrow 10$). This is true in particular when the reorganization of other charged group around the specific ion pair are taken into account.[28] Thus, the optimal ε_p for PDLD/S treatments of charge–charge interactions is larger than the ε_p values that reproduce the self-energies of isolated charges, and the optimal value of this ε_p values cannot be determined apriori. Apparently, as much as charge–charge interaction are concerned, the use of ε_{eff} is as ad hoc as the use of ε_p in the PDLD/S model. Furthermore, the use of large ε_{eff} gives similar results of those obtained by the PDLD/S-LRA model with an explicit consideration of the counter ions and with $\varepsilon_p = 6$. In view of these facts, we prefer to examine here what range of ε_{eff} best reproduces the observed ΔpK_{app} and to see whether the use of a universal ε_{eff} has a predictable value.

With the above philosophy in mind we examined the dependence of the ΔpK_{app} obtained by the PDLD/S-LRA on the values of ε_p and ε_{eff} (Table III). For simplicity, we presented the results obtained with a distance independent ε_{eff} (this corresponds to $\mu = \infty$, $\varepsilon_{eff} = 1 + \varepsilon'$). As seen from the table, we obtained poor results with small values of ε_{eff}, and the optimal results were obtained with ε_{eff} between 40 and 80. We also obtained optimal results with $\varepsilon' = 60$ and $\mu = 0.18$, but these results are not given because of space limitations.

With the procedure used in Table III we also tried to reproduce ΔpK_{app}^{obs} by different models, using in each case the optimal ε_p and ε_{eff}. The corresponding results, which are summarized in Table IV, are similar to those reported in Table II, where in each case we can identify the same problems considered in the discussion of Table II.

Another way of examining different models is to try to see how they perform with a single value of ε_p, where in each case we choose the ε_p that appears most frequently in Table III. Such an analysis is presented in Figures 6, 7, and 8. As seen from Figure 6 the MTK(S) model can produce reasonable results for groups that are destabilized by the protein by using large ε_p. However, when the protein stabilizes ionized groups, the MTK(S) model with large ε_p gives simply incorrect results. The PDLD/S(A) and PDLD/S(B) models give reasonable but not quantitative results with $\varepsilon_p = 4$ and $\varepsilon_p = 8$, respectively. Finally, the PDLD/S-LRA model gives quantitative results with $\varepsilon_p = 4$, except in cases where the ionized group is very unstable in the environment it has in the unionized form (e.g., SNaseK66 and SNaseE66). In such cases the PDLD/S-LRA simulations do not reproduce sufficient water penetrations and we have to use $\varepsilon_p = 6$. The significance of this will be discussed in The Nature of ε_p.

Tight Ion-Pairs

For the sake of completeness, it is also important to consider here tight ion pairs. In such cases it is safer to treat the charge–charge interaction explicitly, by including the given ionized group and its counter ion in the PDLD/S-LRA treatment. The results of such a treatment are given in Table V where we consider explicitly several tight ion pairs. For comparison, we also consider the same pairs by estimating the corresponding ΔG_{ij} using Eq. 17 and the optimal ε_{eff} (Table VI). As seen from Table V we can reproduce the observed ΔpK_a for tight ion pairs by using the PDLD/S-LRA approach, while treating the ion pairs explicitly. This is done while representing the solvent molecules by Langevin dipoles. It is of interest that an alternative PB attempt to treat the Asp-His ion pair in T4

TABLE IV. Calculated ΔpK_{app} for Different Models[†]

System	Born (∞)	TK	MTK	MTK/S	PDLD/S-A	PDLD/S-B	PDLD/S-LRA	ΔpK_{app}^{obs}
thrxD26(o)	2.9 (20, 40)	2.9 (−4, 40)	3.4 (20, 80)	3.9 (6, 80)	2.9 (4, 40)	3.9 (4, 80)	3.5 (4, 80)	3.5
thrxD26(r)	6.3 (10, 80)	4.4 (−4, 80)	4.9 (10, 80)	4.9 (6, 80)	5.4 (4, 8)	4.8 (6, 80)	5.7 (4, 80)	5.3
lysE35	1.5 (20, 80)	2.0 (−10, 80)	2.0 (10, 8)	1.5 (8, 80)	1.5 (4, 80)	2.0 (4, 80)	1.8 (4, 80)	1.8
T4lysE105	1.5 (20, 80)	1.5 (−40, 80)	0.1 (4, 80)	0.5(20, 80)	0.5 (8, 80)	1.0 (8, 80)	1.6 (4, 80)	1.5
T4lysK102	−4.1 (20, 40)	−5.1 (−4, 80)	−4.6 (10, 80)	−5.1 (8, 80)	−4.1 (4, 80)	−4.6 (6, 80)	−4.3 (4, 80)	−3.9
eraH6	−3.2 (20, 80)	−3.5 (−10, 80)	−2.7 (20, 80)	−3.2 (8, 80)	−4.2 (4, 40)	−3.7 (20, 40)	−3.8 (4, 80)	−3.8
subInH43	−1.6 (20, 80)	−2.2 (−8, 80)	−3.2 (10, 80)	−4.2 (8, 80)	−2.2 (4, 80)	−2.2 (8, 80)	−3.9 (4, 80)	−3.4
cytcH26	−3.2 (20, 80)	−3.2 (−30, 80)	−3.7 (6, 80)	−3.2 (8, 40)	−3.2 (4, 80)	−3.7 (8, 80)	−3.2 (6, 80)	−3.4
SNaseK66	−5.2 (10, 80)	−3.2 (−4, 40)	−4.1 (10, 80)	−4.5 (8, 80)	−4.1 (4, 40)	−5.1 (8, 80)	−4.5 (6, 80)	−4.9
SNaseE66	5.8 (10, 80)	3.4 (−6, 80)	4.5 (8, 80)	3.8 (6, 80)	3.0 (4, 80)	5.0 (6, 80)	3.8 (6, 80)	4.3
RiboD76	−3.8 (−60, 40)	−3.8 (10, 40)	−3.1 (−25, 80)	−3.5 (−15, 80)	−3.3 (20, 40)	−3.0 (80, 20)	−3.2 (4, 40)	−3.4

[†]The different models are defined in the text. The optimal ε_p and ε_{eff} for each model are given in brackets (ε_p, ε_{eff}).

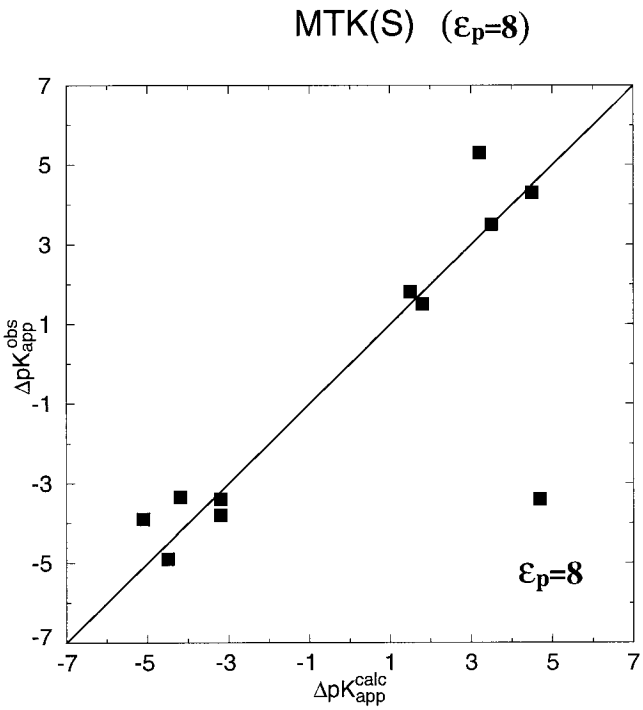

Fig. 6. The correlation between the calculated and observed ΔpK_a obtained by the MTK(S) model, with $\varepsilon_p = 8$, for our benchmark.

Lysozyme[22] could only reproduce the observed interactions by introducing explicit water molecules near the ionized residues (the orientation to these molecules were determined by MD relaxation run). This cannot be used as a general PB procedure because the position of the solvent molecules is frequently unknown and because the orientation of the explicit solvent molecules should be determined by the LRA approach. At any rate, we can treat tight ion pairs within the PDLD/S-LRA approach by using $\varepsilon_p = 6$.

Now looking at Table VI, we find that we can even treat tight ion pairs, to a reasonable approximation while using Eq. 17 in macroscopic estimate of ΔG_{ij}. However, this requires us to use different ε_p in different cases and to use the lower limit of ε_{eff} (i.e., $\varepsilon_{eff} \cong 20$). Similar results are also obtained with the ε_{eff} of Eq. 18 and with $\varepsilon' = 60$ and $\mu = 0.18$. In view of these results, we recommend treatment of tight ion pairs by using the PDLD/S-LRA treatment and considering the pairs explicitly.

It might be useful to comment here on the general issue of ion pairs in proteins. The relevant microscopic energies of such systems were first analyzed in our early studies,[3,37,57] where it was repeatedly emphasized that ion pairs are not stable in low dielectric environments. Similar points were made subsequently by other workers (e.g., Refs. 66, 67). We also emphasized that ion pairs are stabilized by proteins (relative to water) when the protein provides the proper reorganized polar environment.[3,37,68,69] In this contest it was also pointed out that the effective dielectric constant for the interaction between ions in proteins is quite large,[3,57] although it is smaller than the corresponding dielectric constant in water.[68] This point has some relevance to recent studies of the role of ion pairs in proteins stability. For example, Hendsch and Tidor[67] examined different ion pairs and discussed their role in protein stability. However, these works used PB approach with a low value of ε_p. This might have led to nonquantitative results. That is, in the case of T4 lysozyme the calculated energies for $Asp70^{\circ} \cdots His31^{+} \rightarrow Asp70^{-} \cdots His31^{+}$ and for $Asp70^{-} \cdots His31^{\circ} \rightarrow Asp70^{-} \cdots His31^{+}$ were −0.69 kcal/mol and −0.77 kcal/mol, respectively. This should be compared to the corresponding observed values (−4.7 and −1.9 kcal/mol) or the values obtained in the present study (−4.7 and −2.2 kcal/mol). Similarly, the estimate of 10 kcal/mol distabilization of the Glu11-Arg45 ion pair in T4 lysozyme seems to be a significant overestimate relative to the result of ~3 kcal/mol obtained by the current PDLD/S-LRA study. It is significant that the $Asp70^{-} \cdots His31^{+}$ ion pair does not appear to destabilize the protein. That is, the energy of moving the ion pair from infinite separation in water to the protein site (relative to the corresponding energy for a nonpolar pair) was found here to be around zero compared to the 3.46 kcal/mol obtained in Ref. 67. The origin of difference between the two studies can be traced in part to the estimate of the stabilizing effect of the protein permanent dipoles (the $V_{q\mu}$ term in this work and $\Delta G_{protein}$ in Ref. 67). The ~−5 kcal/mol $V_{q\mu}$ contribution found by the PDLD/S-LRA approach correspond to a contribution of only ~−0.26 kcal/mol in Ref. 67. This might be due to the

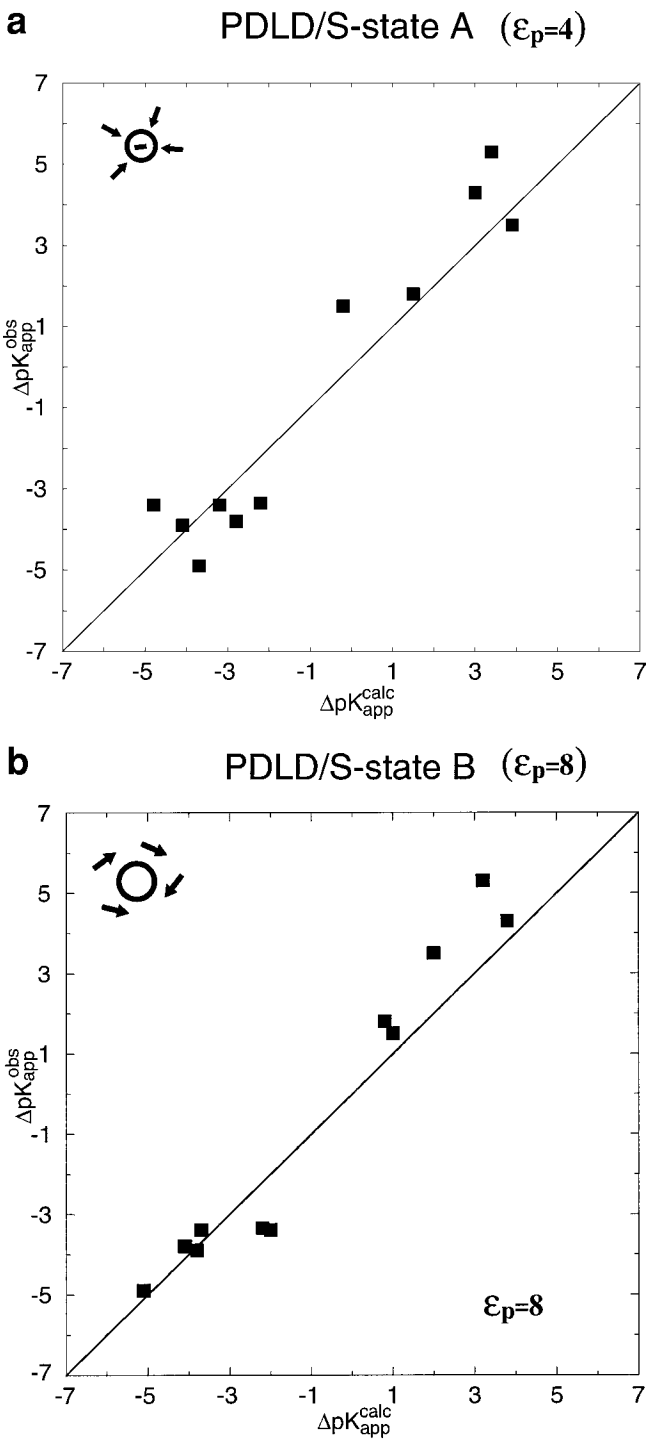

Fig. 7. **A:** The correlation between the calculated and observed ΔpK_a obtained by the PDLD/S model with an average over the configuration generated with the charged forms of the residues studied. Here the best results are obtained with $\varepsilon_p = 4$. **B:** The correlation between the calculated and observed ΔpK_a obtained by the PDLD/S model with an average over the configuration generated with the uncharged forms of the residues studied. Here the best results are obtained with $\varepsilon_p = 8$.

use of an approach that does not allow polar groups to reorient in response to the charges of the ion pair. It is exactly the stabilizing effect of the protein polar groups that plays a crucial role in stabilizing ion pairs in proteins.[2,3] In any rate, the estimate of the energetics of ion pairs depends crucially on the dielectric constant used and models that do not consider the protein relaxation explicitly must use larger ε_p than the PDLD/S-LRA model.[28]

THE NATURE OF ε_P

The main findings of the previous sections are summarized in Figure 9, where we plot the optimal values of ε_p for the different models used. As seen from the figure and from the more detailed results presented in Tables II and III the optimal value of ε_p depends on the model used. This finding might seem as a questionable conclusion to readers who are accustomed to the view that macroscopic models have a universal meaning. This might also look strange to some workers who are experienced with microscopic statistical mechanics, where ε is evaluated in a unique way from the fluctuations of the total dipole moment of the system (see below). Many workers accept that ε_p should depend on the position of the relevant region in the protein (e.g., Ref 70). Yet, it is not so widely recognized that ε_p has little to do with what is usually considered as the protein dielectric constant. Apparently, as was concluded in Ref. 3, the value of the dielectric constant of proteins is entirely dependent on the way used to define this constant and on the model used.

Warshel and coworkers[32,71] pointed out that the dependence of ε_p on the model used can be best realized by asking what is included explicitly in the given model. That is, when all is included explicitly, $\varepsilon = 1$; when all but induced dipoles are included explicitly, $\varepsilon = 2$ (Ref. 3); and when the solvent is not included explicitly, $\varepsilon > 40$ (although this is a very bad model). When the protein permanent dipoles are included explicitly but their relaxation (the protein reorganization) and the protein induced dipoles are considered implicitly, the value of ε_p is not well defined. In this case ε_p should be between 4 and 6 for dipole charge interaction and >10 for charge–charge interactions.[28,72]

One may try to argue that there is only one "proper" dielectric constant, which is the one obtained from the fluctuations of the average dipole moment.[6,27,30,32,73] However this protein dielectric constant ($\varepsilon_p = \bar{\varepsilon}$) is not a constant because it depends on the site considered.[27,32] In many cases $\bar{\varepsilon}$ is significantly larger than the traditional value ($\bar{\varepsilon} \cong 4$) deduced from measurements of dry proteins and peptide powders,[74,75] or from simulations of the entire protein rather than specific regions (e.g., Ref. 27). The larger than expected value of $\bar{\varepsilon}$ was attributed to the fluctuations of ionized side chains.[27,24] However, careful simulations that included the reaction field of the solvent gave $\bar{\varepsilon} \cong 10$ in and near protein active sites, even in the absence of the fluctuations of the ionized residues. It has been clearly shown that the fluctuations of the protein polar groups and internal water molecules contribute significantly to the increase in $\bar{\varepsilon}$. That is, physically consistent studies[32] of $\bar{\varepsilon}$ near ionizable residues indicated that the contributions to $\bar{\varepsilon}$ from the protein permanent dipoles is relatively large. Studies that found a small

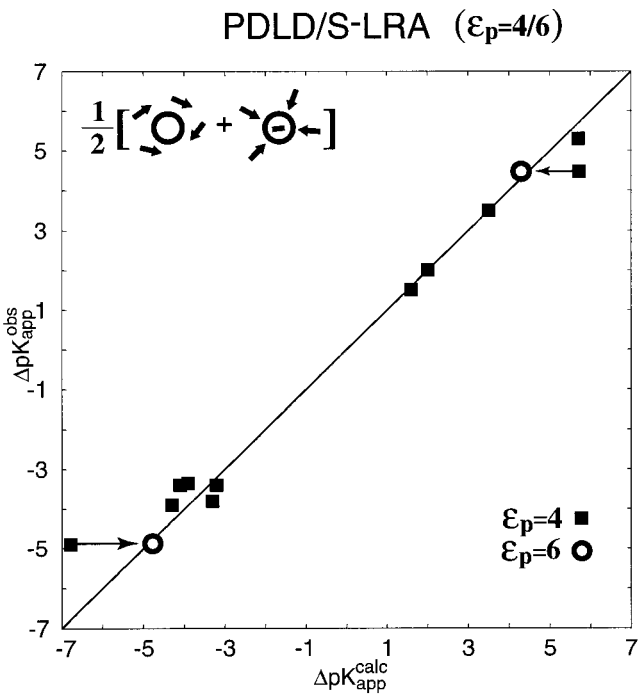

Fig. 8. The correlation between the calculated and observed ΔpK_a obtained by the PDLD/S-LRA model. Here the best results are obtained with $\varepsilon_p = 4$, except for SNaseK66 and SNaseE66, where we used $\varepsilon_p = 6$.

TABLE V. ΔpK_a Values for Ion Pairs Where the Counter Ion is Treated Explicitly[†]

Residue	ΔpK_{int}^{calc}	ΔpK_{int}^{obs}	ΔpK_{app}^{calc}	ΔpK_{app}^{obs}
RiboD76	−2.4 (6)	−2.6	−3.4 (6, 80)	−3.4
RiboH40	1.1 (6)	0.9	1.6 (6, 80)	1.4
T4lysD70	−0.8 (6)	−1.7	−2.6 (6, 80)	−3.4
T4lysH31	1.7 (6)	2.2	2.1 (6, 40)	2.6

[†]In this case pK_{int} includes the effect of the counter ion. In brackets the optimal ε_p and ε_{eff} (here ε_{eff} is only used for the interaction between the ion pair and its surrounding ionized groups).

contributions to $\bar{\varepsilon}$ from protein polar groups[75] did not treat the reaction field from the solvent correctly (see discussion in Ref. 32).

Although the nature of $\bar{\varepsilon}$ is of interest, it is not so relevant to electrostatic energies in proteins. Here one is interested in the energies of charges in their specific environment and the ways available for a reliable and effective evaluation of these energies. Unfortunately, $\bar{\varepsilon}$ does not tell us in a unique way how to determine the ε_p of semimacroscopic models. For example, obtaining $\varepsilon_p = 1$ in a fully microscopic model, or $\varepsilon_p = 2$ in a model with implicit induced dipoles has nothing to do with the corresponding $\bar{\varepsilon}$. The best way to realize this point is to think on charges in a water sphere (our hypothetical protein) surrounded by water. In such a model $\bar{\varepsilon} \cong 80$, whereas microscopic models of the same system with implicit induced dipoles will be best described by using $\varepsilon_p = 2$. Of course, one may argue that the entire concept of a dielectric constant is invalid in heterogenous environment of proteins.[41] However, because fully microscopic models are still not giving sufficiently precise results, it is very useful to have reasonable estimates using implicit models and in particular semimacroscopic models. Thus, it is justified to look for optimal ε_p values after realizing, however, what these parameters really mean.

TABLE VI. ΔpK_a Values for Ion Pairs Where the Counter Ion is Treated Macroscopically[†]

Residue	ΔpK_{int}^{calc}	ΔpK_{int}^{obs}	ΔpK_{app}^{calc}	ΔpK_{app}^{obs}
RiboD76	−1.3 (4)	−1.8	−3.2 (4, 40)	−3.4
RiboH40	1.2 (8)	−1.1	1.3 (8, 20)	1.4
T4lysD70	3.1 (4)	3.2	−2.1 (4, 15)	−3.4
T4lysH31	−0.5 (20)	−0.1	2.3 (20, 20)	2.6

[†]In brackets the optimal ε_p and ε_{eff}.

The use of a consistent semimacroscopic model such as the PDLD/S-LRA does not guarantees that the corresponding ε_p will approach a universal value. For example, in principal the PDLD/S-LRA model should involve $\varepsilon_p = 2$, because all effects except the effect of the protein induced dipoles are considered explicitly. However, the configurational sampling by the LRA approach is not perfect. The protein reorganization energy is probably captured to a reasonable extent,[76] but the change in water penetration on ionization of charged residues is probably not reproduced in an accurate way. This problem is practically serious when we have ionized groups in nonpolar sites in the interior of the proteins. In such cases we have significant changes in water penetration[21] during the ionization process, but these changes are unlikely to be reproduced by standard simulations times. This is the reason why we obtain $\varepsilon_p = 6$ for SNaseK66 and SNaseE66.

The fact that ε_{eff} for charge–charge interactions is large has been pointed out by several workers.[57,61,77] However, this important observation was not always analyzed with the proper microscopic perspective. Mehler and coworkers[25,61] argued that $\varepsilon_{eff}(r)$ is a sigmoid function with a large value at relatively short distances based on classical studies of $\varepsilon(r)$ in water.[78–80] Similarly, it has been assumed by Jönsson and coworkers[77] that electrostatic interactions in proteins can be described by using a large ε_{eff} for charge–charge interactions. However, although we completely agree that ε_{eff} is large in many cases and we repeatedly advanced this view,[3] we believe that the reasons for this are much more subtle. That is, the finding of a particular behavior of ε in water might be not so relevant to the corresponding behavior in proteins (in principle ε_{eff} in proteins can be very different from ε_{eff} in water). Here the remarkable reason why ε_{eff} is large, even in protein interiors, was first rationalized by our early work.[2,3] This was done by pointing out the compensation of charge–charge interactions and solvation energy in proteins.[3] It was also concluded that the large ε_{eff} reflects the fact that the protein resistance to local unfolding is relatively small. Thus, the rearrangement of the protein dipoles and water penetration can compensate very effectively for the increase in energy in charge separation processes (e.g., see Fig. 4 in Ref. 28). It seems to us that the understanding of this crucial compensation effect is essential for understand-

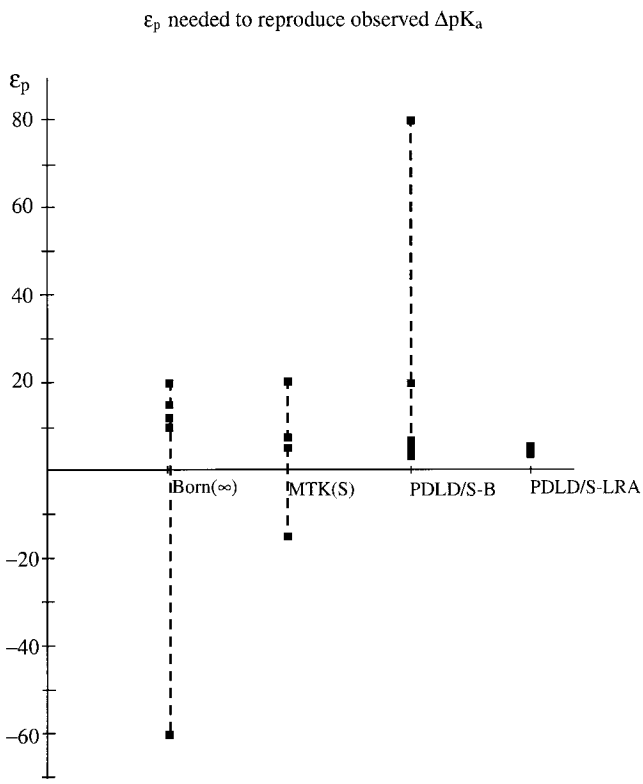

Fig. 9. The correlation between the optimal ε_p and the model used.

ing of the nature of ε_{eff} in proteins (see Ref. 28 for a recent analysis of this issue).

CONCLUSIONS

This work explored the meaning of the dielectric constants of proteins and the consistency of different electrostatic models. The use of a discriminative benchmark, which only considered large pK_a shifts, appeared to provide a major insight about the nature of different electrostatic models. It was shown that some models, that do not provide the correct ΔpK_a values in such a benchmark, seem to work remarkably well in less discriminative benchmarks.

The use of our benchmark allows us to demonstrate the assertion[3] that the dielectric "constant" of proteins depends in a critical way on its definition and on the specific model used. Usually, the more implicit is the model the larger is the dielectric constant needed. However, macroscopic models cannot capture correctly the physics of electrostatic energies in proteins. Thus, the less microscopic is the model, the less universal is the value of the corresponding ε_p.

This work showed that the use of $\varepsilon_{eff} \geq 20$ give reasonable results when combined with a proper treatment of the corresponding self-energies. This important point might require further clarification. That is, the fact that large ε_{eff} gives reasonable results for charge–charge interactions has been pointed out repeatedly.[3,28,57,61] However, it has also been stated[3,57] that ε_{eff} should be used only for the changes in pK_a values due to charge–charge interactions and that the self-energy of each ionizable group must be evaluated with the proper microscopic or semimacroscopic treatment. This point has been sometimes ignored in studies that obtained reasonable results using large ε_{eff} and no self-energy term (see discussion in Ref. 81). However, obtaining reasonable results in such cases simply reflect the use of a nondiscriminative benchmark. Of course, as shown here, the self-energy term is crucial in cases with large ΔpK_{int} (see Examining Macroscopic and Semimacroscopic Models). Some may argue that the fact that proteins do not behave like a low dielectric spheres and do not involve very large disolvation penalties indicated that the self-energy term is not really needed. This is simply incorrect; the large disolvation penalties predicted for nonpolar spheres are the *exact* results for such models. However, it is hard for proteins to retain nonpolar environment around charged groups without undergoing a partial unfolding and allowing a penetration of water molecules.[37] Ignoring the self energy-term would prevent us from understanding this effect.

In recent years it has been frequently stated (e.g., Ref. 24) that $\varepsilon_p \cong 20$ should be used in macroscopic models instead of $\varepsilon_p \cong 4$, which was commonly used in most earlier PB studies. However, the need to use large ε_p is a result of the attempt to describe both self-energies and charge–charge interactions by the same ε_p. As shown in this work, the self-energy is reproduced most consistently by ε_p between 4 and 8 (depending on the semimacroscopic model used) once we remove the requirement that the same ε_p should be used for charge–charge interactions and for self-energies. The finding that ε_p can be ~4 does not mean that the "correct" ε_p value is small because presumably the "correct" dielectric of proteins is around 4. It merely indicates that when the protein permanent dipole, protein reorganization energy, and water penetration are taken into account, we can use a small ε_p, and eventually use $\varepsilon_p = 1$ when all contributions are treated explicitly and accurately.

The finding that ε_{eff} is usually quite large also holds for ionized groups in proteins interiors. In such cases the solvent contribution to ε_{eff} (which is correctly taken into account in PB methods) is rather small and $\varepsilon_{eff} \cong \varepsilon_p$. Assuming that $\varepsilon_p \cong 4$ will lead to $\varepsilon_{eff} \cong 4$, when one deals with internal ions, and to a very large ΔG_{ij}. Such large ΔG_{ij} are, however, inconsistent with mutation experiments (e.g., Ref. 82). Apparently ε_{eff} is large even in protein interiors, because it reflects the reorganization of the protein polar groups and water penetration and not only the effect of the solvent around the protein. Preliminary attempts to include the protein relaxation in PB model have been reported by Alexov and Gunner[83] (who adapted some of our LRA ideas but still implement it in a restricted local minimization approach). Obviously, it is entirely "legal" to combine the PB approaches with the LRA as is done routinely with the PDLD/S approach in the program MOLARIS.[44,65]

It is important to comment here on some cases where ε_{eff} is significantly smaller than our generic estimate. This is the case in some alosteric proteins (e.g., the change in

Ras-RAF interaction on conversion of GTP to GDP[17]), where the electrostatic interactions appear to be transmitted over large distances. In such cases we are dealing with relatively rigid motion of protein units (see schematic description in Fig. 2 of Ref. 84) which is not compensated so much by the surrounding.

Finally, we would like to prevent the possible impression that simple implicit models are not useful. The opposite is true; simple models, such as the one with large ε_{eff}, are extremely effective. It is not justified, however, to assume that because a given model reproduces some benchmarks, this model is generally correct. It is even less justified to assume that the dielectric constant of a given implicit model has a simple universal meaning that follows from some "textbook" electrostatic concept (e.g., $\bar{\varepsilon}$). Apparently, semimacroscopic models that may look as rigorous models are in fact based on phenomological scaling factors. Nevertheless, knowing the proper scaling factor (i.e., ε_p) for different cases provides a powerful tool for modeling biomolecules.

REFERENCES

1. Perutz MF. Electrostatic effects in proteins. Science 1978;201: 1187.
2. Warshel A. Electrostatic basis of structure-function correlation in proteins. Accts Chem Res 1981;14:284–290.
3. Warshel A, Russell ST. Calculations of electrostatic interactions in biological systems and in solutions. Q Rev Biophys 1984;17:283–421.
4. Warshel A. Computer modeling of chemical reactions in enzymes and solutions. New York: John Wiley & Sons; 1991.
5. Sharp KA, Honig B. Electrostatic interactions in macromolecules: theory and applications. Annu Rev Biophys Biophys Chem 1990;19:301.
6. Nakamura H. Roles of electrostatic interaction in proteins. Q Rev Biophys 1996;29:1–90.
7. Matthew JB. Electrostatic effects in proteins. Annu Rev Biophys Biophys Chem 1985;14:387–417.
8. Hilvert D. Critical analysis of antibody catalysis. Annu Rev Biochem 2000;69:751–793.
9. Parson WW, Chu ZT, Warshel A. Electrostatic control of charge separation in bacterial photosynthesis. Biochim Biophys Acta 1990;1017:251.
10. Gunner M, Nichols A, Honig B. Electrostatic potential in rhodopseudomonas viridis reaction centers: implications for the driving force and directionality of electron transfer. J Phys Chem 1996; 100:4277–4291.
11. Sham Y, Muegge I, Warshel A. Simulating proton translocations in proteins: probing proton transfer pathways in the rhodobacter sphaeroides reaction center. Proteins 1999;36:484–500.
12. Okamura MY, Feher G. Proton transfer in reaction centers from photosynthetic bacteria. Annu Rev Biochem 1992;61:861–896.
13. Åqvist J, Warshel A. Energetics of ion permeation through membrane channels: solvation of na+ by gramicidin a. Biophys J 1989;56:171.
14. Åqvist J, Luzhkov V. Ion permeation mechanism of the potassium channel. Nature 2000;404:881.
15. Lee FS, Chu ZT, Bolger MB, Warshel A. Calculations of antibody-antigen interactions: microscopic and semi-microscopic evaluation of the free energies of binding of phosphorylcholine analogs to mcpc603. Prot Eng 1992;5:215–228.
16. Simonson T, Archontis G, Karplus M. Continuum treatment of long-range interactions in free energy calculations. application to protein-ligand binding. J Phys Chem B 1997;101:8349–8362.
17. Muegge I, Schweins T, Warshel A. Electrostatic contributions to protein-protein binding affinities: application to rap/raf interaction. Proteins 1998;30:407–423.
18. Glennon TM, Villà J, Warshel A. How does gap catalyze the gtpase reaction of ras? A computer simulation study. Biochemistry 2000;39:9641–9651.
19. Russell ST, Warshel A. Calculations of electrostatic energies in proteins; the energetics of ionized groups in bovine pancreatic trypsin inhibitor. J Mol Biol 1985;185:389.
20. Warshel A, Sussman F, King G. Free energy of charges in solvated proteins: microscopic calculations using a reversible charging process. Biochemistry 1986;25:8368.
21. Garcia-Moreno B, Dwyer JJ, Gittis AG, Lattman EE, Spencer DS, Stites WE. Experimental measurement of the effective dielectric in the hydrophobic core of a protein. Biophys Chem 1997;64:211–224.
22. Honig B, Sharp K, Sampogna R, Gunner MR, Yang AS. On the calculation of pK_a values in proteins. Proteins 1993;15:252–265.
23. Del Buono GS, Figueirido FE, Levy RM. Intrinsic pK_a values of ionizable residues in proteins: an explicit solvent calculation for lysozyme. Proteins 1994;20:85–97.
24. Antosiewicz J, McCammon JA, Gilson MK. Prediction of ph-dependent properties of proteins. J Mol Biol 1994;238:415–436.
25. Mehler EL, Guarnieri F. A self-consistent, microspcopic modulated screened coulomb potential approximation to calculate ph-dependent electrostatic effects in proteins. Biophys J 1999;75: 3–22.
26. Warshel A, Papazyan A. Electrostatic effects in macromolecules: fundamental concepts and practical modeling. Curr Opin Struct Biol 1998;8:211–217.
27. Simonson T, Brooks CL. Charge screening and the dielectric constant of proteins: insights from molecular dynamics. J Am Chem Soc 1996;118:8452–8458.
28. Sham YY, Muegge I, Warshel A. The effect of protein relaxation on charge–charge interactions and dielectric constants of proteins. Biophys J 1998;74:1744–1753.
29. Dwyer JJ, Gittis AG, Karp AD, Lattman EE, Spencer DS, E SW, Garcia-Moreno BE. High apparent dielectric constants in the interior of a protein reflect water penetration. Biophys J 2000;79: 1610–1620.
30. Smith PE, Brunne RM, Mark AE. Dielectric properties of trypsin inhibitor and lysozyme calculated from molecular dynamics simulations. J Phys Chem 1993;97:2009–2014.
31. Mehler EL. The lorentz-debye-sack theory and dielectric screening of electrostatic effects in proteins and nucleic acids. In: Murray JS, Sen K, editors. Molecular electrostatic potentials. New York: Elsevier; 1996. p 371–406.
32. King G, Lee FS, Warshel A. Microscopic simulations of macroscopic dielectric constants of solvated proteins. J Chem Phys 1991;95:4366–4377.
33. Churg AK, Warshel A. Control of redox potential of cytochrome c and microscopic dielectric effects in proteins. Biochemistry 1986; 25:1675.
34. Stephens PJ, Jollie DR, Warshel A. Protein control of redox potentials of iron-sulfur proteins. Chem Rev 1996;96:2491.
35. Åqvist J. Calculation of absolute binding free energies for charged ligands and effects of long-range electrostatic interactions. J Comp Chem 1996;17:1587.
36. Warshel A, Sussman F, Hwang J-K. Evaluation of catalytic free energies in genetically modified proteins. J Mol Biol 1988;201: 139–159.
37. Warshel A. Calculations of enzymic reactions: calculations of pka, proton transfer reactions, and general acid catalysis reactions in enzymes. Biochemistry 1981;20:3167–3177.
38. Sham YY, Chu ZT, Warshel A. Consistent calculations of pka's of ionizable residues in proteins: semi-microscopic and macroscopic approaches. J Phys Chem B 1997;101:4458–4472.
39. Bashford D, Karplus M. pka's of ionizable groups in proteins: atomic detail from a continuum electrostatic model. Biochemistry 1990;29:10219–10225.
40. Warshel A, Naray-Szabo G, Sussman F, Hwang J-K. How do serine proteases really work? Biochemistry 1989;28:3629.
41. Warshel A, Levitt M. Theoretical studies of enzymatic reactions: dielectric, electrostatic and steric stabilization of the carbonium ion in the reaction of lysozyme. J Mol Biol 1976;103:227–249.
42. Lee FS, Warshel A. A local reaction field method for fast evaluation of long-range electrostatic interactions in molecular simulations. J Chem Phys 1992;97:3100–3107.
43. Kollman P. Free energy calculations: applications to chemical and biochemical phenomena. Chem Rev 1993;93:2395–2417.
44. Lee FS, Chu ZT, Warshel A. Microscopic and semimicroscopic calculations of electrostatic energies in proteins by the POLARIS and ENZYMIX programs. J Comp Chem 1993;14:161–185.

45. Sham YY, Warshel A. The surface constrained all atom model provides size independent results in calculations of hydration free energies. J Chem Phys 1998;109:7940–7944.
46. Warshel A, Chu ZT. Calculations of solvation free energies in chemistry and biology. In: Truhlar DG, Cramer CJ, editors. ACS Symposium Series: Structure and Reactivity in Aqueous Solution. Characterization of Chemical and Biological Systems. Washington, DC: ACS; 1994. p 72–93.
47. Figueirido F, Del Buono GS, Levy RM. On the finite size corrections to the free energy of ionic hydration. J Phys Chem B 1997;101:5622–5623.
48. Hummer G, Pratt LR, Garcia AE. Ion size and finite-size corrections for ionic-solvation free energies. J Chem Phys 1997; 107:9275–9277.
49. Kirkwood JG. Theory of solutions of molecules containing widely separated charges with special application to zwitterions. J Chem Phys 1934;2:351–361.
50. Alper H, Levy RM. Dielectric and thermodynamic response of generalized reaction field model for liquid state simulations. J Chem Phys 1993;99:9847–9852.
51. Warshel A. Calculations of chemical processes in solutions. J Phys Chem 1979;83:1640–1650.
52. King G, Warshel A. A surface constrained all-atom solvent model for effective simulations of polar solutions. J Chem Phys 1989;91: 3647–3661.
53. Brooks CL, Karplus M. Deformable stochastic boundaries in molecular dynamics. J Chem Phys 1983;79,6312.
54. Beglov D, Roux B. Finite representation of an infinite bulk system: solvent boundary potential for computer simulations. J Chem Phys 1994;100:9050–9063.
55. Åqvist J. Comment on "transferability of ion models". J Phys Chem 1994;98:8252–8255.
56. Zhou HX. Control of reduction potential by protein matrix: lesson from a spherical protein model. J Biol Inorg Chem 1997;2:109–113.
57. Warshel A, Russell ST, Churg AK. Macroscopic models for studies of electrostatic interactions in proteins: limitations and applicability. Proc Natl Acad Sci USA 1984;81:4785.
58. Tanford C, Kirkwood JG. Theory of protein titration curves. i. general equations for impenetrable spheres. J Am Chem Soc 1957;79:5333.
59. Li YK, Kuliopulos A, Mildvan AS, Talalay P. Environments and mechanistic roles of the tyrosine residue of δ^5-3-ketosteroid. Biochemistry 1993;32:1816–1824.
60. Beroza P, Fredkin MY, Okamura MY, Feher G. Protonation of interacting residues in a protein by a monte carlo method: application to lysozyme and the photosynthetic reaction center of rhodobater sphaeroides. Proc Natl Acad USA 1991;88:5804–5808.
61. Mehler EL, Eichele G. Electrostatic effects in water-accessible regions of proteins. Biochemistry 1984;23:3887–3891.
62. Edinger SR, Cortis C, Friesner RA. Solvation free energies of peptides: comparison of approximate continuum solvation models with accurate solution of the poisson-boltzmann equation. J Phys Chem 1997;101:1190–1197.
63. Luzhkov V, Warshel A. Microscopic models for quantum mechanical calculations of chemical processes in solutions: LD/AMPAC and SCAAS/AMPAC calculations of solvation energies. J Comp Chem 1992;13:199.
64. Still CS, Tempczyrk A, Hawley RC, Hendrickson T. Semianalytical treatment of solvation for molecular mechanics and dynamics. J Am Chem Soc 1990;112:6127–6129.
65. Chu ZT, Villà J, Schutz CN, Strajbl M, Warshel A. 2001. (In preparation)
66. Honig BH, Hubbell WL. Do "salt bridges" exist in membrane proteins. Biophys J 1983;41:203.
67. Hendsch ZS, Tidor B. Do salt bridges stabilize proteins? a continuum electrostatic analysis. Protein Sci 1994;3:211–226.
68. Warshel A. Energetics of enzyme catalysis. Proc Natl Acad Sci USA 1978;75:5250–5254.
69. Hwang J-K, Warshel A. Why ion pair reversal by protein engineering is unlikely to succeed. Nature 1988;334:270.
70. Demchuk E, Wade RC. Improving the continuum dielectric approach to calculating pK_a values of ionizable groups in proteins. J Phys Chem 1996;100:17373–17387.
71. Warshel A, Åqvist J. Electrostatic energy and macromolecular function. Annu Rev Biophys Chem 1991;20:267.
72. Muegge I, Schweins T, Langen R, Warshel A. Electrostatic control of gtp and gdp binding in the oncoprotein p21 ras. Structure 1996;4:475–489.
73. Simonson T, Perahia D, Brünger AT. Microscopic theory of the dielectric properties of proteins. Biophys J 1991;59:670–690.
74. Harvey S, Hoekstra P. Dielectric relaxation spectra of water adsorbed on lysozyme. J Phys Chem 1972;76:2987–2994.
75. Gilson M, Honig B. The dielectric constant of a folded protein. Biopolymers 1986;25:2097–2119.
76. Muegge I, Qi PX, Wand AJ, Chu ZT, Warshel A. The reorganization energy of cytochrome c revisited. J Phys Chem B 1997;101: 825–836.
77. Penfold R, Warwicker J, Jönsson B. Electrostatic models for calcium binding proteins. J Phys Chem B 1998;108:8599–8610.
78. Debye PJW, Pauling L. The inter-ionic attraction theory of ionized solutes. IV. The influence of variation of dielectric constant on the limiting law for small concentrations. J Am Chem Soc 1925;47:2129–2134.
79. Webb TJ. The free energy of hydration of ions and the electrostriction of the solvent. J Am Chem Soc 1926;48:2589–2603.
80. Hill TL. The electrostatic contribution to hindered rotation in certain ions and dipolar ions in solution iii. J Chem Phys 1944;12:56–61.
81. Mehler EL, Warshel A. Comment on "a fast and simple method to calculate protonation states in proteins." Proteins 2000;40:1–3.
82. Alden RG, Parson W, Chu Z, Warshel A. Calculations of electrostatic energies in photosynthetic reaction centers. J Am Chem Soc 1995;117:12284–12298.
83. Alexov E, Gunner M. Incorporating protein conformational flexibility into the calculation of ph-dependent protein properties. Biophys J 1997;72:2075.
84. Warshel A, Weiss RM. Energetics of heme-protein interactions in hemoglobin. J Am Chem Soc 1981;103:446.
85. Chivers PT, Prehoda KE, Volkman FB, Kim BM, Markley JL, Raines TR. Microscopic pK_a value of *Enscherichia coli* thioredoxin. Biochemistry 1997;36:14985–14991.
86. Katti SK, LeMaster DM, Eklund H. Crystal structure of thioredoxin from *escherichia coli* at 1.68 a resolution. J Mol Biol 1990;212:167.
87. Cohen JS, Fisher WR, Schechter AN. Spectroscopic studies on the conformation of cytochrome c and apocytochrome c. J Biol Chem 1974;249:1113–1118.
88. Bushnell GW, Louie GV, Brayer GD. High-resolution three-dimensional structure of horse heart cytochrome c. J Mol Biol 1990;214:585.
89. Stites WE, Gittis AG, Lattman EE, Shortle D. In a staphylococcal nuclease mutant the side-chain of a lysine replacing valine 66 is fully buried in the hydrophobic core. J Mol Biol 1991;221:7.
90. Dobson CM, Refield C, Bartik K. Measurement of the individual pka values of acidic residues of hen and turkey lysozymes by teo dimensional 1h nmr. Biophys J 1994;66:1180–1184.
91. Diamond R. Real-space refinement of the structure of hen white lysozyme. J Mol Biol 1974;82:371.
92. Pajura P, McIntosh LP, Wozniak JA, Matthews BW. Perturabation of trp 138 in t4 lysozyme by mutations at gln used to correlate changes in structure, stability, solvation, and spectroscopic properties. Proteins 1993;15:401–412.
93. Doa-pin S, Anderson DE, Baase WA, Dahlquist FW, Matthews BW. Structural and thermodynamic consequences of buring a charged residue within the hydrophobic core of t4 lysozyme. Biochemistry 1991;30:11521–11529.
94. Anderson DE, Becktel WJ, Dahlquist FW. ph-induced denaturation of proteins: a single bridge contributes 3–5 kcal/mol to the free energy of folding of t4 lysozyme. Biochemistry 1990;29:2403–2408.
95. Inagaki F, Miyazawa T, Hori H, Tamiya N. Conformation of erabutoxins a and b in aqueous solution as studied by nuclear magnetic resonance and circular dichroism. Eur J Biochem 1978;89:433–442.
96. Smith JL, Corfield PWR, Hendrickson WA, Low BW. Refinement at 1.4 angstroms resolution of a model of erabutoxin b. treatment of ordered solvent and discrete disorder. Acta Crystallogr Sect A 1988;44:357.
97. Fujii S, Akasaka K, Hatano H. Acid denaturation steps of *Streptomyces* subtilisin inhibitor. J Biochem 1980;88:789–796.
98. Suzuki T. Structural modulation of the protein proteinase inhibitor ssi (streptomyces subtilisin inhibitor). Forthcoming.

99. Giletto A, Pace CN. Buried, charged, non-ion-paired aspartic acid 76 contributes favorably to the conformational stability of ribonuclease. Biochemistry 1999;38:13379–13384.
100. Martinez-Oyenedel J, Choe HW, Heinemann U, Saenger W. J Mol Biol 1991;222:335–352.
101. Inagaki F, Kawano Y, Shimada I, Takahashi K, Miyazawa T. Nuclear magnetic resonance study on the microenvironments of histidine residues of ribonuclease t_1 and carboxymethylated ribonuclease t_1. J Biochem 1981;89:1185–1195.

APPENDIX A

Because the PDLD/S formulation plays a central role in our discussion, we provide here the relevant derivation. Our starting point is Figure 2 where the charging free energy $\Delta G_{a\to b}$ is given by

$$\Delta G_{a\to b} = \Delta G_{a\to d} + \Delta G_{d\to c} + \Delta G_{c\to b} \tag{A1}$$

We start by considering $\Delta G_{a\to d}$. The contributions to this term from the solvated charge is easily evaluated by

$$\begin{aligned}\Delta G_q^{\varepsilon_p} - \Delta G_q^w &= -\left(\frac{166}{\bar{a}}\right)\left[\left(1-\frac{1}{\varepsilon_p}\right)-\left(1-\frac{1}{\varepsilon_w}\right)\right]\\ &= -\Delta G_q^w\left(\frac{1}{\varepsilon_p}-\frac{1}{\varepsilon_w}\right)\Big/\left(1-\frac{1}{\varepsilon_w}\right)\\ &\simeq -\Delta G_q^w\left(\frac{1}{\varepsilon_p}-\frac{1}{\varepsilon_w}\right)\end{aligned} \tag{A2}$$

where ΔG_q^w is the self-energy of the given charge in water (the ΔG_{self}^w of Eq. 3), and $\Delta G_q^{\varepsilon_p}$ is the solvation of the charge in a medium with $\varepsilon = \varepsilon_p$. Here we express ΔG_q^w by the Born's formula and then determine the relevant Born's radius $\bar{a}$ from the actual (microscopically calculated) ΔG_q^w. The contribution from the change in the solvation of the protein ($\Delta G_p^{\varepsilon_p} - \Delta G_p^w$) is now evaluated in a similar way. This is done by

$$\begin{aligned}\Delta G_p^{\varepsilon_p}(q=0) - \Delta G_p^w(q=0) \simeq &-\left(\frac{166q^2}{\bar{b}}\right)\left(\frac{1}{\varepsilon_w}-\frac{1}{\varepsilon_p}\right)\\ &-\left(\frac{166\mu^2}{b^3}\right)\left[\left(\frac{2\varepsilon_p-2}{2\varepsilon_p+1}\right)-\left(\frac{2\varepsilon_w-2}{2\varepsilon_w+1}\right)\right]\end{aligned} \tag{A3}$$

where ΔG_p^w is the solvation energy of the entire protein with its ionizable group in its indicated charge state, b is the Born's radius of the protein, q is the total protein charge, and μ is the total dipole of the protein.

Using the relationship

$$\left(\frac{2\varepsilon-2}{2\varepsilon+1}\right) = \left(1-\frac{1}{\varepsilon}\right)\left(\frac{1}{1+1/2\varepsilon}\right) = \left(1-\frac{1}{\varepsilon}\right)f(\varepsilon) \tag{A4}$$

where $f(\varepsilon) = (1 + 1/2\varepsilon)^{-1}$, we can write Eq. A3 as

$$\begin{aligned}\Delta G_p^{\varepsilon_p}(q=0) - \Delta G_p^w(q=0) \simeq \\ -\left(\frac{166q^2}{b}+\frac{166\mu^2}{b^3}f(\varepsilon)\right)\left(\frac{1}{\varepsilon_w}-\frac{1}{\varepsilon_p}\right)\end{aligned} \tag{A5}$$

For ΔG_p^w (where $f(\varepsilon) \simeq 1$) we can certainly write

$$\begin{aligned}\Delta G_p^w &\simeq -\left(\frac{166q^2}{b}+\frac{166\mu^2}{b^3}\right)\left(1-\frac{1}{\varepsilon_w}\right)\\ &= -\left(\frac{166q^2}{b}+\frac{166\mu^2}{b^3}\right).\end{aligned} \tag{A6}$$

Now we can write for $\varepsilon_p \geq 6$

$$\Delta G_p^{\varepsilon_p}(q=0) - \Delta G_p^w(q=0) \cong \Delta G_p^w\left(\frac{1}{\varepsilon_p}-\frac{1}{\varepsilon_w}\right). \tag{A7}$$

When ε_p is <6 we should modify the scaling of ΔG_p^w by the above $f(\varepsilon_p)$. This is done conveniently in our simulation studies by evaluating in addition to ΔG_p^w, also $\Delta G_p^{\varepsilon=2}$ and using these two values and Eq. A5 to obtain an interpolated value for b and $f(\varepsilon)$. The additional calculation for $\varepsilon_p = 2$ is very fast. That is, in the case of small ε_p we can use a noniterative approach with a grid of dipoles with the corresponding polarizability and with a screening constant that represents the dipole–dipole interactions.[3] However, even without the $f(\varepsilon)$ correction, the contribution from the μ^2 term of the protein largely cancels when we also include the $\Delta G_{c\to d}$ term. Furthermore, the physics of scaling by ε_p is as qualitative as is the nature of ε_p. Thus, we use in our qualitative discussion the approximation

$$\Delta G_{a\to d} = -(\Delta G_p^w(q=0) + \Delta G_q^w)\left(\frac{1}{\varepsilon_p}-\frac{1}{\varepsilon_w}\right) \tag{A8}$$

$\Delta G_{d\to c}$ is evaluated by taking the microscopic contribution from the interaction between the protein residual charges to the ionized group (this contribution is called here $\Delta V_{q\mu}^p$, and it becomes $\Delta G_{q\mu}^p$ upon proper LRA averaging) and dividing it by ε_p. Thus, we can write

$$\Delta V_{c\to d} = \frac{\Delta V_{q\mu}^p(q_i=\bar{q}_i)}{\varepsilon_p}. \tag{A9}$$

Here we use $\Delta V_{c\to d}$, rather than $\Delta G_{c\to d}$, to indicate that we are dealing with an effective potential. The simple expression of Eq. A9 can be used in this step, because all of our system is immersed in a continuum with $\varepsilon = \varepsilon_p$. Finally, $\Delta G_{c\to d}$ is evaluated in the same way as $\Delta G_{a\to d}$. Summing the three terms in Eq. A1 leads to our effective potential, which is written as

$$\begin{aligned}\Delta V_{pdld/s,i}^{w\to p} \simeq [\Delta\Delta G_p^w(q_i=0 \to q_i=\bar{q}_i) - \Delta G_{q,i}^w]\left(\frac{1}{\varepsilon_p}-\frac{1}{\varepsilon_w}\right)\\ + \frac{\Delta V_{q\mu}^p(q_i=\bar{q}_i)}{\varepsilon_p}\end{aligned} \tag{A10}$$

where the $\Delta\Delta G_p^w$ term represents the change in the microscopic solvation energy of the entire protein plus its bound ionizable group upon changing the charge of this group from zero to $\bar{q}$.